NAVAL POSTGRADUATE SCHOOL
MONTEREY, CALIFORNIA

THESIS

SPRAY GENERATION FROM FREE AND HALF-FREE JETS

by

Rajan Vaidyanathan

March 1999

Thesis Advisor: T. Sarpkaya

Approved for public release; distribution is unlimited.

REPORT DOCUMENTATION PAGE			Form Approved OMB No. 0704-0188
Public reporting burden for this collection of information is estimated to average 1 hour per response, including the time for reviewing instruction, searching existing data sources, gathering and maintaining the data needed, and completing and reviewing the collection of information. Send comments regarding this burden estimate or any other aspect of this collection of information, including suggestions for reducing this burden, to Washington Headquarters Services, Directorate for Information Operations and Reports, 1215 Jefferson Davis Highway, Suite 1204, Arlington, VA 22202-4302, and to the Office of Management and Budget, Paperwork Reduction Project (0704-0188) Washington DC 20503.			
1. AGENCY USE ONLY (Leave blank)	2. REPORT DATE March 1999	3. REPORT TYPE AND DATES COVERED Master's Thesis	
4. TITLE AND SUBTITLE SPRAY GENERATION FROM FREE AND HALF-FREE JETS			5. FUNDING NUMBERS
6. AUTHOR(S) Rajan Vaidyanathan			
7. PERFORMING ORGANIZATION NAME(S) AND ADDRESS(ES) Naval Postgraduate School Monterey CA 93943-5000			8.PERFORMING ORGANIZATION REPORT NUMBER
9. SPONSORING/MONITORING AGENCY NAME(S) AND ADDRESS(ES)			10.SPONSORING/MONITORING AGENCY REPORT NUMBER
11. SUPPLEMENTARY NOTES The views expressed in this report are those of the authors and do not reflect the official policy or position of the Department of Defense or the U.S. Government.			
12a. DISTRIBUTION/AVAILABILITY STATEMENT Approved for public release; distribution is unlimited.			12b. DISTRIBUTION CODE

13. ABSTRACT (maximum 200 words)

This is an experimental investigation of the ligament and drop formation at the free surface of wall jets, flowing over sand-roughened plates, and on unbounded two-dimensional jets, discharging into atmosphere. Experiments were conducted with both fresh and simulated sea water. Measurements were made with several high-speed imagers and a pulsating laser system and analyzed through the use of appropriate software. The wall-jet Reynolds number ranged from $3.5x10^4$ to $8.5x10^4$, the Froude number from 15 to 30, and the Weber number from 3,000 to 7,500. The positions of the transition and primary breakup as well as the characteristics of the ligament forest and droplets were determined from the digitized images and interpreted in terms of the characteristics of the turbulent boundary layer and a phenomenological model based on our observations and measurements. The emphasis has been on the physics of the phenomenon rather than on the development of empirical relationships.

14. SUBJECT TERMS Spray, Drops, Jets, Bow sheets, Liquid sheets, Turbulent boundary layers			15.NUMBER OF PAGES 74
			16.PRICE CODE
17.SECURITY CLASSIFICATION OF REPORT Unclassified	18.SECURITY CLASSIFICATION OF THIS PAGE Unclassified	19.SECURITY CLASSIFICATION OF ABSTRACT Unclassified	20.LIMITATION OF ABSTRACT UL

THIS PAGE LEFT INTENTIONALLY BLANK

Approved for public release; distribution is unlimited

SPRAY GENERATION FROM FREE AND HALF-FREE JETS

Rajan Vaidyanathan
Lieutenant, United States Navy
B.S., Punjabi University ,1987

Submitted in partial fulfillment of the
requirements for the degree of

MASTER OF SCIENCE IN MECHANICAL ENGINEERING

from the

NAVAL POSTGRADUATE SCHOOL

March 1999

Author: Rajan Vaidyanathan
Rajan Vaidyanathan

Approved by:
T. Sarpkaya, Thesis Advisor

Terry R. McNelley, Chairman,
Department of Mechanical Engineering

THIS PAGE LEFT INTENTIONALLY BLANK

ABSTRACT

This is an experimental investigation of the ligament and drop formation at the free surface of wall jets, flowing over sand-roughened plates, and on unbounded two-dimensional jets, discharging into atmosphere. Experiments were conducted with both fresh and simulated sea water. Measurements were made with several high-speed imagers and a pulsating laser system and analyzed through the use of appropriate software. The wall-jet Reynolds number ranged from 3.5×10^4 to 8.5×10^4, the Froude number from 15 to 30, and the Weber number from 3,000 to 7,500. The positions of the transition and primary breakup as well as the characteristics of the ligament forest and droplets were determined from the digitized images and interpreted in terms of the characteristics of the turbulent boundary layer and a phenomenological model based on our observations and measurements. The emphasis has been on the physics of the phenomenon rather than on the development of empirical relationships.

THIS PAGE LEFT INTENTIONALLY BLANK

TABLE OF CONTENTS

THIS PAGE LEFT INTENTIONALLY BLANK

LIST OF FIGURES

LIST OF SYMBOLS

Af	filament area
Ddr	drop diameter
Df	effective filament diameter, Af/Lf
Fr	jet Froude number, $U/(gho)^{½}$
g	gravity
ho	mean jet thickness at leading edge of plate
k	mean roughness height
Lf	filament length
Re	jet Reynolds number, Uho/ν
We	jet Weber number, $\rho U^2 ho/\sigma$
x	streamwise axis
Z	Ohnesorge number, $\mu/(\rho ho\sigma)^{1/2}$
ν	kinematic viscosity of fluid
μ	dynamic viscosity of fluid
ρ	density of fluid
σ	surface tension of fluid

THIS PAGE LEFT INTENTIONALLY BLANK

ACKNOWLEDGEMENTS

There have been three significant turning points in my life thus far: first when I joined the Navy, second when I married my wife Preeti and the third is this project that I worked on with Distinguished Professor Sarpkaya as a part of my graduate education.

To him I owe my sincerest gratitude for enhancing my education with his technical guidance and wisdom. His constant tutelage was a source of strength and inspiration to me. Not a day went by when I did not learn something new from him.

I would like to thank my wife from the bottom of my heart for the long hours of absence she endured while I was working on this project. Her constant support, encouragement, and patience always inspired me. I would also like to thank my family whose blessings have always been with me. Finally, I would like to thank Sri Satya Sai Baba for giving me this opportunity.

THIS PAGE LEFT INTENTIONALLY BLANK

I. INTRODUCTION

Spray is the cause of several major problems for a ship. The most important ones are the icing around the forward perimeter of the hull, reduced equipment operability or damage, and the enhancement of ship's radar cross-section. The motivation for the present investigation is to understand the physics of the spray created by the bow of a ship as it moves through and/or slams into the oncoming waves.

The problem of drop formation has developed in many directions and presents different points of view and different goals for various disciplines. The fact that it continues to attract the attention and energy of impressively large numbers of researchers attests to its technological importance and, just as importantly, to its intellectual challenge.

The drop formation in a circular liquid jet has attracted the most mathematical and experimental interest for obvious reasons. The sprays generated from spray roots and their rupture into smaller particles have been of major practical interest in the field of combustion. There are many other applications where a continuum becomes a two- or multi-phase flow through drop dynamics (agriculture, naval architecture, irrigation, decorative fountains, ship-plunging, ink-jet printing, perfumery, deuterium microspheres and laser fusion, chemical warfare, just to name a few). The impetus for the present research comes from the need to understand the physics of spray formation at the free surface of turbulent free jets and wall jets and, subsequently, the breakup of bow sheets into fine spray. The latter may help to reduce the visual and radar signatures of ships subjected to the accumulation of water mass on exterior surfaces.

A critical review of the extensive literature (Merrill 1998) has shown that the breakup of jets and sheets depends strongly not only on the conditions governing their creation but also on the conditions surrounding their subsequent evolution under the influence of several competing internal/external influences such as turbulence, gravity, surface tension, liquid-sheet geometry, surface shear, roughness of the contact surface(s), velocity distribution in the sheet, temperature distribution in the jet, pressure fluctuations within

and outside the liquid sheet, acoustic excitation, external flows (e.g., wind), intentionally imposed disturbances, and foreign particles (e.g., air, dust). It is generally agreed that eddies accelerated by the internal motion of the fluid tear into irregular shapes and give rise to ligaments (threads) and droplets. The ligaments may initially appear as large undefined volumes of water or nearly transparent sheets. These shapes then continue to rupture into smaller particles until the surface tension forces inhibit them from further disintegration under the prevailing environmental conditions.

The investigation described herein deals with the breakup of two types of flows, namely that of a two-dimensional liquid free jet (free at both the top and bottom) and a wall jet with a single free surface. It must be emphasized that the only apparent difference between the much-studied "wall jet" and the one described herein is that whereas the "wall jet" discharges into a medium of identical fluid, the liquid or free wall jet is bounded by a smooth or rough wall below and a free surface above (air/water interface). The resulting flow is intended to simulate the inception of bow sheet/spray flows for an observer on board the ship. In the present experiments, the jet issues (a) from a nozzle and (b) from a streamlined gate at the upstream end of a recirculating free-surface water tunnel. In both cases the jet is maintained in a steady state as long as desired for a detailed measurement of the characteristics of ligaments, droplets, and bubbles. No attempt has been made to develop empirical relations between particular characteristics of the flow and the Weber number, Reynolds number, Froude number, and the relative roughness.

The investigation of free and half free (wall-bounded) jet, though quite specific, still raises a large number of fundamental questions some of which are undoubtedly common to all spray phenomena: How important is the nozzle shape (two dimensional or axisymmetric) on the subsequent evolution of the jet? If turbulence is ultimately responsible for the ejection of the lumps of fluid from the jet body, then what is responsible for the turbulence in a wall-jet with free surface: External aerodynamic excitation, internal instability and the wall of the partially wall-bounded flow, or both? How is the free-surface/turbulence interaction modified by ejections? How does that

modification manifest itself along the jet? How does the shape of the free surface (curvature, shear) affect the mass, momentum, and vorticity flux across the free surface? Considering the fact that in internal turbulent flows more momentum is transferred from the flow to the walls, how does the free surface affect the partitioning of the jet-momentum flux between the bottom wall, the free surface, and the jet? What role does the condition of the wall surface play in the ejection-sweep cycle or in the relative magnitudes of the components of the stress tensor? Does roughness enhance the mass, momentum, and vorticity flux towards and out of the free surface? Clearly, this is a very complex two-phase flow problem, requiring the understanding of the internal as well as the surface flow, even for a wall-bounded and relatively well-defined jet geometry.

Partial answers to some of the foregoing questions have been provided by several investigators prior to 1977: Phinney (1973), McCarthy and Molloy (1974), and Hoyt and Taylor (1977a and 1977b) to name a few, and more recently by Wu et al (1995) and Dai et al (1998) towards the quantification of the characteristics of spray phenomena on annular liquid wall jets about axisymmetric rods. These have shown that the qualitative features of flows over spillways, plunge pools, open water waves, and axisymmetric rods are quite similar. Their observations and measurements have also suggested that turbulence generated on the wall propagates across the flow and reaches the interface and roughens the free surface. This laminar-turbulent transition at the air/water interface is followed by a region of turbulent breakup where a forest of ligaments rise above the free surface. Some, but not all, of these ligaments give rise to one or more droplets. Subsequently, the free-surface activity gradually subsides due to loss of momentum. The positions of the transition and primary breakup as well as the character of the ligament forest can be affected by trip wires, local or uniformly-distributed roughness, and possibly by aerodynamic effects.

The question of the origin of turbulence and the aerodynamic effects were addressed by a number of investigators to include Hoyt and Taylor (1977a and 1977b), Wu et al (1995), Dai et al (1998) and Finley et al (1966). It has been concluded that the origin of turbulence is the same as in all internal flows (instability of the flow and the walls) and

not the relative motion at the liquid/air interface. In other words, the aerodynamic effects do not play measurable roles in turbulence generation and do not appear to interact with the spray generation. However, the question of how turbulence selectively accelerates and ejects parcels of fluid across the liquid/air interface remains unclear. Equally unclear is the profound effect of roughness in ligament generation and of the air bubbles created within the jet by the entrainment of air carried by the ligaments and droplets falling back on the free surface. One rather obvious reason for this is the lack of detailed velocity and turbulence measurements in free wall jets. For research conducted on turbulent boundary layers, the reader is referred to Feindt (1957), Klebanoff (1954), Ligrani et al (1979), Lord Rayleigh (1945), Pimenta et al (1975), Raupach (1981) and Schlichting (1987). In spite of its major importance, there has never been an experiment with a liquid wall jet, with ligaments and spray, where the distributions of the mean as well as the instantaneous flow fields and the complete Reynolds stress tensor were measured at numerous sections downstream from the nozzle. What is measured is for very low-Froude-number flows (Finley et al 1966) where the free surface exhibits nothing more than small irregular fluctuations. There are, to be sure, numerous hot-wire and LDV measurements in wall jets (air into air or water into water) and in closed conduits (pipes and rectangular channels). Some of these measurements are accompanied by numerical simulations (DNS, LES, RANS) at relatively low Reynolds numbers.

II. APPARATUS AND PROCEDURES

A two-dimensional nozzle of aspect ratio of 32 (Fig. 1) was attached to a large U-shaped water tunnel (10 m wide and 7.5 m high) at a suitable location along one of its two vertical towers (Sarpkaya 1977 and 1986). The upstream face of the nozzle (facing the tunnel wall) was carefully streamlined so as to provide a smooth entrance into the nozzle (Fig. 2). It was known early on (Dombrowski and Fraser 1954) that the nozzle design has a significant impact on the characteristics of the resulting jet and that data from various sources cannot be compared on the basis of Reynolds and Weber numbers alone. The nozzle shown in Figs. 1 and 2 embodies all of the past recommendations (McCarthy and Molloy 1974, Hoyt and Taylor 1977a and 1977b, Dombrowski and Fraser 1954 and Rouse and Abol-Fetouh 1950), (e.g., a gradual geometric transition, continued acceleration, earlier transition on the walls and a thinner turbulent boundary layer).

The jet exited from the nozzle upon the removal of a cylindrical gate (Fig. 4) and flowed, after a short free flight (about 80 mm), over the horizontal test plate. The jet surface had a fine-grained texture on emergence due to the turbulent surface layer. Only for relatively low velocities did the jet have an extremely smooth clear surface, as if it were frozen. In either case, however, the jet was essentially non-turbulent by the time it reached the edge of the plate.

The discharge was collected in a trough and then pumped back into the opposite tower of the U-shaped tunnel as shown in Fig. 3. A foam divider, sandwiched between two heavy wire screens, was inserted near the mid-length of the horizontal section of the tunnel. These precautions have indeed assured that the flow entering into the nozzle was free from disturbances, as verified by flow visualization with dye (food coloring). With this arrangement it was easy to maintain constant jet velocities from 3 m/s to 6.5 m/s indefinitely. Suffice it to note that the use of a nearly ideal nozzle, long observation and measurement times, and reliance on high-speed video (HSV), and Laser-Induced Florescence (LIF) made the entire apparatus particularly unique for the investigation

under consideration. The additional advantages of the system were the relative ease with which the test plates (smooth or rough) can be interchanged, bodies of special interest can be mounted, and the flow can be illuminated and photographed.

The basic test plate was a 33 cm wide and 120 to 180 cm long smooth Plexiglas sheet, mounted horizontally and rigidly on adjustable supports. For the free jet experiments, the length of the plate used was 63.5 cm and the ramp angle was adjusted to the desired value using the adjustable supports mentioned above. The upstream edge of each plate was beveled with a sharp edge at an angle of 30 degress from the horizontal. The elevation of the sharp-edge of the horizontal plate was positioned carefully so as to capture only the top 6 mm of the 8.5 mm jet. Plates were sand-roughened carefully to achieve the desired relative mean roughness height of $k/h_o = 0.06$. Some plates had as many as five strategically-located dye holes along a line about 60 mm from the edge of the plate for flow visualization. The use of tripping wires or tripping sand-strips were considered and even subjected to trial runs. However, the realization that the resulting turbulent motion at any section of a smooth flat plate may neither be representative of the bow/sheet interaction nor accurately depict the ejection-sweep processes in liquid wall jets with a free surface, led to the use of only smooth or only uniformly-roughened surfaces with no tripping wires. It is a well-known fact that the near-wall region is characterized by a randomly recurring burst cycle (the violent ejection of the low-speed fluid towards the free surface and the down sweep of higher-speed fluid towards the wall). Roughness renders the mean flow three dimensional in the roughness sublayer, gives rise to higher energy ejections not existing in smooth wall flows, rapidly increases the thickness of the jet by extracting larger momentum, and thus changes not only the character of the ejections and sweeps but also the interaction of the coherent structures with the free surface. Since the free-surface structures (including ligaments and droplets) are an outgrown manifestation of the bursting process in the wall region, the behavior of the turbulent motion generated by a uniformly-roughened surface cannot be duplicated by that of a trip-wire-generated turbulent motion over a smooth wall. There are, to be sure,

circumstances where trip wires serve the intended purposes well (e.g., precipitate transition, delay separation).

Instrumentation consisted of several high-speed cameras with frame rates from 250 frm/s to 1,000 frm/s (with shutter speeds from 1/250 to 1/10,000 sec). The recordings of the jet surface, ligaments, droplets, and the scales inscribed on the plate were made along the jet (within a 1.6 m long and 30 mm wide centrally-located strip, along the longitudinal axis of the plate) through the use of proper lenses and back and front lighting. This assured that a single ligament or a droplet could be tracked during its lifetime, from its creation to its return to the body of the jet, without being obscured by the shadows of ligaments in neighboring planes.

The video images were first carefully reviewed to identify a number of representative ligaments (with or without droplets) whose motion could be traced with little or no ambiguity. The diameter, volume, tip velocity, and lifespan of ligaments, the wave-number of the axisymmetric disturbances, time of droplet formation, droplet size and velocity, free surface velocity, the temporal mean of the local jet thickness, in addition to the distances to the region of transition and roughness, to the region of surface distortions and ligaments, and to the region of ligaments and droplets were evaluated through the use of a suitable software (Optimas-MA). It is of some importance to note that the characteristic diameter of a ligament was evaluated by drawing a contour around the ligament and automatically evaluating the enclosed area above the free surface and, therefrom, the characteristic diameter and volume.

The determination of the ligament length and diameter involves some uncertainty because the beginning of the ligament is not precisely definable (due to surface distortions) and the assumption of axisymmetry of the ligament cannot always be ascertained. High-speed video images taken directly from above the jet as well as the visual observations with a high-speed stroboscope have shown that well-defined ligaments were almost always nearly axisymmetric. Nevertheless, the experimental uncertainties cannot be lowered to less than about 20 percent primarily due to scale

effects, highly turbulent nature of the flow, uniqueness of each ligament, and the sampling limitations.

The wall-jet Reynolds number ranged from $3.5x10^4$ to $8.5x10^4$, the Froude number from 15 to 30, and the Weber number from 3,000 to 7,500. Experiments were conducted using fresh water and simulated sea water. Table 1 below provides a summary of all the experiments conducted and their relevant parameters.

Jet Type	Ramp Angle	Water type	Location (inches)	ho (mm)	$Rehx10^{-4}$	Fr	We
Half-free	-	Salt	25.0	5.8	3.67	25.8	3095
Half-free	-	Fresh	27.5	14.0	8.57	16.6	7367
Free	10°	Fresh	35.0	5.8	3.57	25.8	3014
Free	15°	Fresh	32.5	5.8	3.57	25.8	3014
Free	10°	Salt	27.5	5.8	3.67	25.8	3095

Table 1. Summary of Experiments.

All experiments were conducted using medium sand roughness with k/ho = 0.06 and a jet inlet velocity of 6.2 m/s. The location at which the data was analysed is measured from the leading edge of the plate. Needless to say, for each experiment conducted, data was recorded starting at 15.0 inches from the leading edge of the plate all the way up to about 40.0 inches at intervals of 2.5 inches. In all cases, the level of 'activity' would reach a maximum at about 25.0 inches and continue on at that level till about 35.0 inches. 'Activity', refers to the process of forming droplets from ligaments. Locations for data analyses were picked judiciously after careful review of the tapes so that only ligaments and droplets that met the criterion mentioned above were tracked.

III. DISCUSSION OF RESULTS

The general characteristics of filaments and droplets have already been described in Merrill's dissertation (1998), based on the work carried out at the Naval Postgraduate School under the direction of Professor Sarpkaya. Here only the results of the additional research will be described in detail. These concern the characteristics of ligaments and droplets as a function of the distance from the point of inception of the wall jets (often referred to as the half-free jets), over plates of relative roughness of k/ho = 0.06, and free jets of both fresh as well as simulated sea water. Furthermore, the nozzle width and hence the jet thickness were increased from 5.8 mm to 14 mm during the tests to asses the effect of changes in the governing parameters defined by

Relative roughness k/ho

Weber number: $We = \rho U^2 ho/\sigma$

Froude number: $Fr = U/(gho)^{1/2}$

Reynolds number: $Re = Uho/\nu$

Ohnesorge number: $Z = \mu/(\rho ho\sigma)^{1/2}$

Although all of the droplets recorded were measured, the present discussion will focus on those formed at the filament tips. Fig. 5 is a sequence of images showing filament necking and subsequent drop formation. Fig. 6 to Fig. 10 show the multitude in characteristics of filaments, and drops formed from these filaments. As noted here and in other studies (Volkert 1980), the majority of the filaments give birth to only one drop at the filament tip. Even for those that form more than one, the "tip drop" is almost always

the first and the largest. The few drops not produced by this process were very small (Ddr ~ 0.25 mm), and their formation appeared to be similar in nature to that of free surface jetting described by Rein (1996).

Obviously, there are a number of additional measurements that could have been taken from the digitized free-surface images. However, here the analysis is directed toward those measurements that appeared to be the best indicators of the filament-formation and droplet-generation mechanisms. Those indicators are the drop size and the length and diameter of the filament. It is believed their measurements give the clearest possible indication of the events causing the drop formation, as well as the energy associated with their vertical motion.

In the ensuing discussion, histograms will be used frequently to compare and contrast the results of a large number of tests. In doing so, each case will be identified by k/ho, We, and Fr since these parameters uniquely define a given type of water jet. It should be noted that the surface tension and viscosity of the simulated seawater are nearly identical to that of fresh water, i.e., only their densities differ by a measurable amount.

Figures 11 and 12 show the normalized filament length for two half-free fresh water jets, differing only in thickness. The Froude number for the thicker jet is about 35 percent smaller than that of the thinner jet. However, its Weber number is more than twice that of the thinner jet. Since the phenomenon of ligament formation is essentially an inertial phenomenon and since the variation of the Weber number is relatively small compared to the ranges that it could acquire, it is clear that smaller Froude number jets will lead to smaller filaments. In fact, Fig. 13, a combination of Figs. 11 and 12, shows that the jet with smaller Froude number gives rise to relatively smaller filaments over a narrower range.

Figures 14 and 15 show the relative filament diameters for the aforementioned jets. A combined plot (Fig. 16) clearly shows that the filaments of the thicker jets (smaller Froude number) results not only in relatively thinner filaments (smaller Df/ho) but also in relatively shorter filaments (Fig. 13), confirming the fact that the ligament

formation is an essentially inertial phenomenon. Equally interesting is the finding that the jets of relatively smaller Froude number are confined not only to smaller values of Lf/ho and Df/ho, but also to a narrower range of the said parameters. This is compensated by the fact that in the said narrow ranges, the percent occurrence of the thinner and shorter filaments is increased. These observations are in conformity with the reasoning that at much smaller Froude numbers the filament formation ceases altogether.

Next, we examine the characteristics of the droplets for the two wall jets discussed above through the use of Figs. 17-19. It is clear, particularly from Fig. 19, that wall jets of smaller Froude numbers, within a relatively narrow range of Weber numbers, yield relatively smaller droplets in smaller regions of Ddr/ho at a relatively larger percentage. Thus, a fitting conclusion to the discussion of Figs. 11-19 is that wall jets of smaller Froude number give rise to shorter filaments and smaller droplets in narrower ranges of the filament length and diameter. However, their frequency of occurrence is somewhat larger. This is, undoubtedly related to the relative size and number of the turbulent eddies in the two jets: lower turbulence in low Fr jets does not provide as much kinetic energy to the eddies for their travel across the jet and ejection from the surface. When it does so, it does it selectively, narrowing the range in which higher percentages of smaller filaments and droplets occur.

Figures 20 through 28 are assigned to a comparison of the characteristics of the filaments and droplets in fresh- and salt-water wall jets of identical k/ho (= 0.06), We (=3014), and Fr (=25.8). Figures 20-22 and Figs. 23-25 show that the relative filament length and the relative filament diameter are larger for the salt water jets even though their percent occurrences are somewhat smaller. Figures 28 shows that the role of the salt water is just as true in the case of the droplet diameter. In summary of the discussion of the wall jets, the emerging fact is that the effect of the salt is to enhance the relative magnitudes of drop diameter and the filament length and diameter. All of the relative increases are accompanied by a reduction in their percent occurrences.

We have so far examined in as much detail as possible the effect of salt on the free-surface structures of wall jets or half-free jets. We will now introduce one new parameter (angle) and remove one restriction (wall). In other words, we will deal with the characteristics of free jets of fresh as well as salt water.

Figures 29-31 show that the relative filament lengths on two free jets (one with and the other without salt), emerging at an angle of 10 degrees from a ramp where a fully-developed boundary layer relaxes quickly and becomes a free jet. Clearly, the effect of the salt is to reduce the filament length relative to that on a free jet at the same angle. This finding holds true as well for the filament diameter and the droplet diameter as seen from Figs. 32-37. Previously, we have seen that the effect of salt on wall jets was to increase the relative magnitudes of the droplet diameter and the filament length and diameter (Figs. 22-28). The apparent conflict raises the following question: Is the difference due to the unbounded or free nature of the jet, the angle of the jet, the effect of salt, or due to the combined effect of all? This question will be resolved through a series of additional comparisons where the said effects are isolated to the extent possible. Figure 38a shows (for fresh water) the relative filament lengths for the wall jet and a 10-degree free jet. Clearly, either the effect of the unbounded nature and/or the effect of the jet angle are profound and the filament lengths are far to the right of those for the wall jet as seen from a comparison of Figs. 22 and 38a. However, it has already been shown (Merrill 1998) that the angle of the wall jet has very little or no effect on the filament and droplet characteristics. In other words, a fresh-water jet on a horizontal plate will yield nearly identical characteristics as that on an inclined plate (here 10 degrees). Thus, it can be concluded that it is the free or unbounded nature of the jet that is responsible for the significant increase in the filament length in the case of the free jet at 10-degree angle. It has been noted in the "Introduction" that in internal flows more momentum is transferred from the flow to the walls. In other words, the momentum available for the formation of the free-surface structures is reduced. In unbounded jets, however, the full momentum of

the fluid is available for the internal as well as surface structures. Thus, unbounded jets yield larger structures.

The use of salt water produces similar but much milder effects on the ligament length as shown in Fig. 38b. In view of this, it is clear that the unboundedness of the jet is far more effective in enhancing the filament characteristics than the presence of salt. It is because of this reason that the effect of the salt appears to decrease the filament characteristics in Fig. 31, 35, and 37. In reality, a comparison of Figs. 38a and 38b shows that the salt enhances the filament characteristics, but not as much as the unbounded nature of the jet. Figures 39a and 39b and Figs. 40a and 40b confirms the foregoing conclusions in terms of the filament and droplet diameters.

Figures 41-46 show an assessment of the effect of the jet angle (10 degrees versus 15 degrees) on the filament characteristics for fresh water. Apparently, the effect in the change of ramp angle is relatively small as far as the filament length and diameter are concerned. However, Figs. 47-49 show that smaller ramp angles gives rise to relatively larger droplets.

It needs to be pointed out that in all of the results discussed in the foregoing the uncertainty in the normalized mean-value characteristics of the filaments and droplets is less than 5 percent. Reducing the coarse-wall Weber number from 3000 to 1600, as done by Merrill (1998), or nearly doubling, as in the present case, has no apparent influence on the characteristics of the free-surface structures. If anything, the reduction of the Weber number reduces the likelihood of long filament formation and vice versa.

It should also be pointed out that the most important contributions of the present investigation have been the quantification of the physical manifestations of the liquid wall jets, the demonstration of the profound effects of the unboundedness of a jet, and the effect of salt on the free-surface structures. Obviously, the reliability of the information obtained is related to the number of individual realizations, which made the data gathering an enormously time-consuming effort. There is no doubt that the structures of the free surface affect the flow beneath, and the underlying characteristics of the flow

affect the structures of the free surface. In fact, one may conclude that the spray problem is the determination of this interaction for smooth, rough and concave or convex walls in supercritical wall jets. In addition to providing a basis for identifying the governing and influencing parameters on jet behavior, the data will be essential for gaining an even deeper insight into the nature of free surface flows if and when numerical simulations become possible. This is so because the phenomena described herein happens on scales of space and time where experimental measurements and visualizations are difficult or impossible. In such cases, numerical simulations, guided by the results presented herein, may be useful inspiration to all interested in free surface flows. However, the nonisotropy of the turbulence and the near impossibility of finding a suitable turbulent model that incorporates the near surface hydro/aerodynamics are an insurmountable task. These characteristics also make it unlikely that any realistic results will be obtained using anything less than a full three-dimensional model.

IV. CONCLUSIONS

The following conclusions are warranted based on the observations and measurements made in this investigation:

- The characteristics of the free-surface structures (filaments and droplets) are of a statistical nature and can best be described in terms of histograms.
- The free surface provides a path for interaction between the above surface events and the internal flow dynamics. This interaction guarantees that the internal flow for half-free jets is fundamentally different not only from that of typical turbulent flows over plane surfaces but also from that of unbounded jets.
- The characteristics of the filaments and droplets (length and diameter, among others) resulting from the wall jets (half-free jets) depend primarily on the relative wall roughness and the Froude number within the range of Weber numbers encountered.
- Wall jets of smaller Froude number give rise to shorter filaments and smaller droplets in narrower ranges of the filament length and diameter, confirming the fact that the ligament formation is essentially an inertial phenomenon.
- There are fundamental differences between the bounded and unbounded jets. The latter invariably gives rise to larger filaments and droplets because the full momentum of the jet is available for the internal as well as the surface structures of the jet. In wall jets (half-free jets), considerable amount of momentum is consumed by the wall and the remaining momentum is shared by the internal and surface structures.
- The presence of salt in water (in amounts to simulate seawater) enhances the physical dimensions of the filaments and droplets. However, The unboundedness of the jet is far more effective in enhancing the filament

characteristics than the presence of salt. All of the relative increases are accompanied by a reduction in their percent occurrences.

- As far as the inclined jets are concerned, it is the free or unbounded nature of the jet that is primarily responsible for the significant increases in the filament length. The effect of jet inclination is relatively small.
- Aerodynamics does not appear to influence the characteristic behavior of the filaments and drops as shown by flow visualizations.
- The most important contributions of the present investigation have been the quantification of the physical manifestations of the liquid half-free and free jets, the demonstration of the profound effects of the unboundedness of a jet, and the effect of salt on the free-surface structures. The data will be essential for gaining an even deeper insight into the nature of free surface flows if and when numerical simulations become possible. This is so because the phenomena described herein happens on scales of space and time where experimental measurements and visualizations are extremely difficult.

APPENDIX

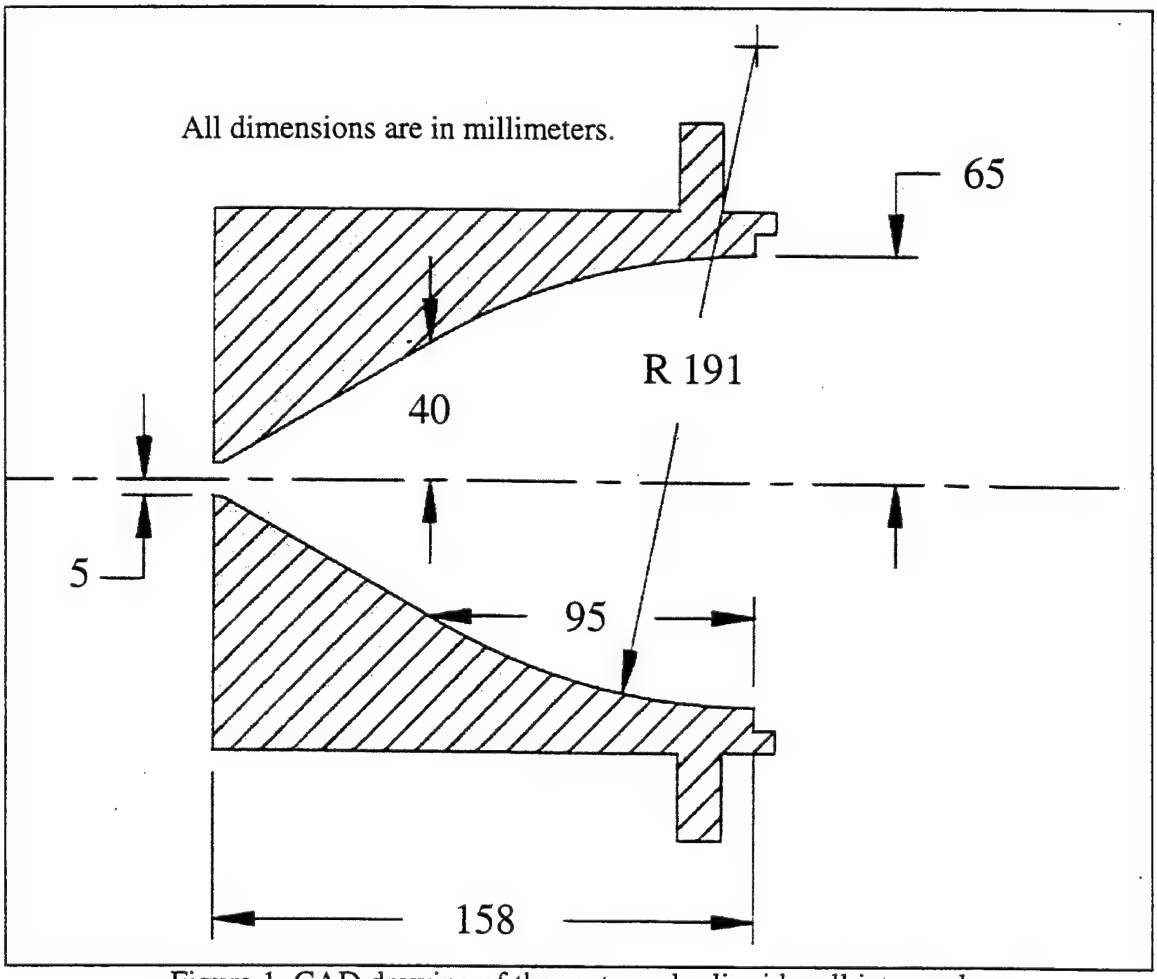

Figure 1. CAD drawing of the rectangular liquid wall jet nozzle.

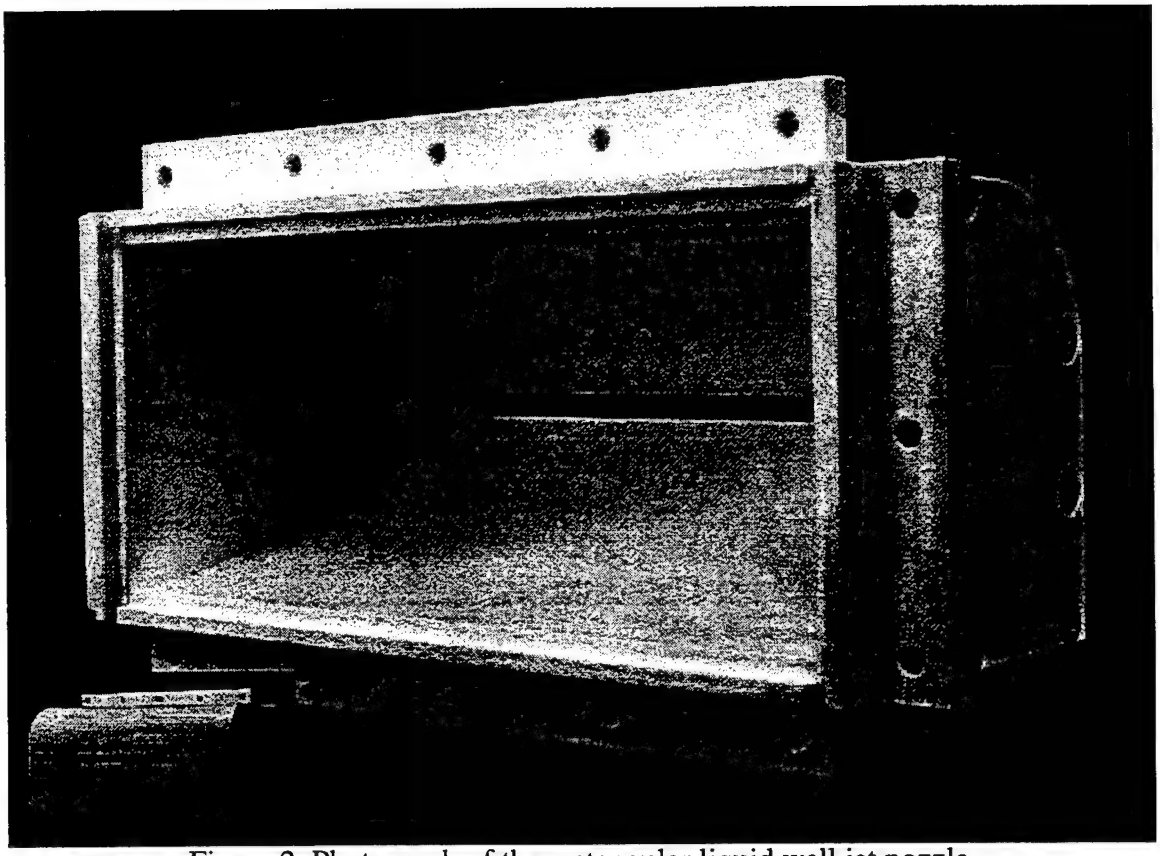

Figure 2. Photograph of the rectangular liquid wall jet nozzle.

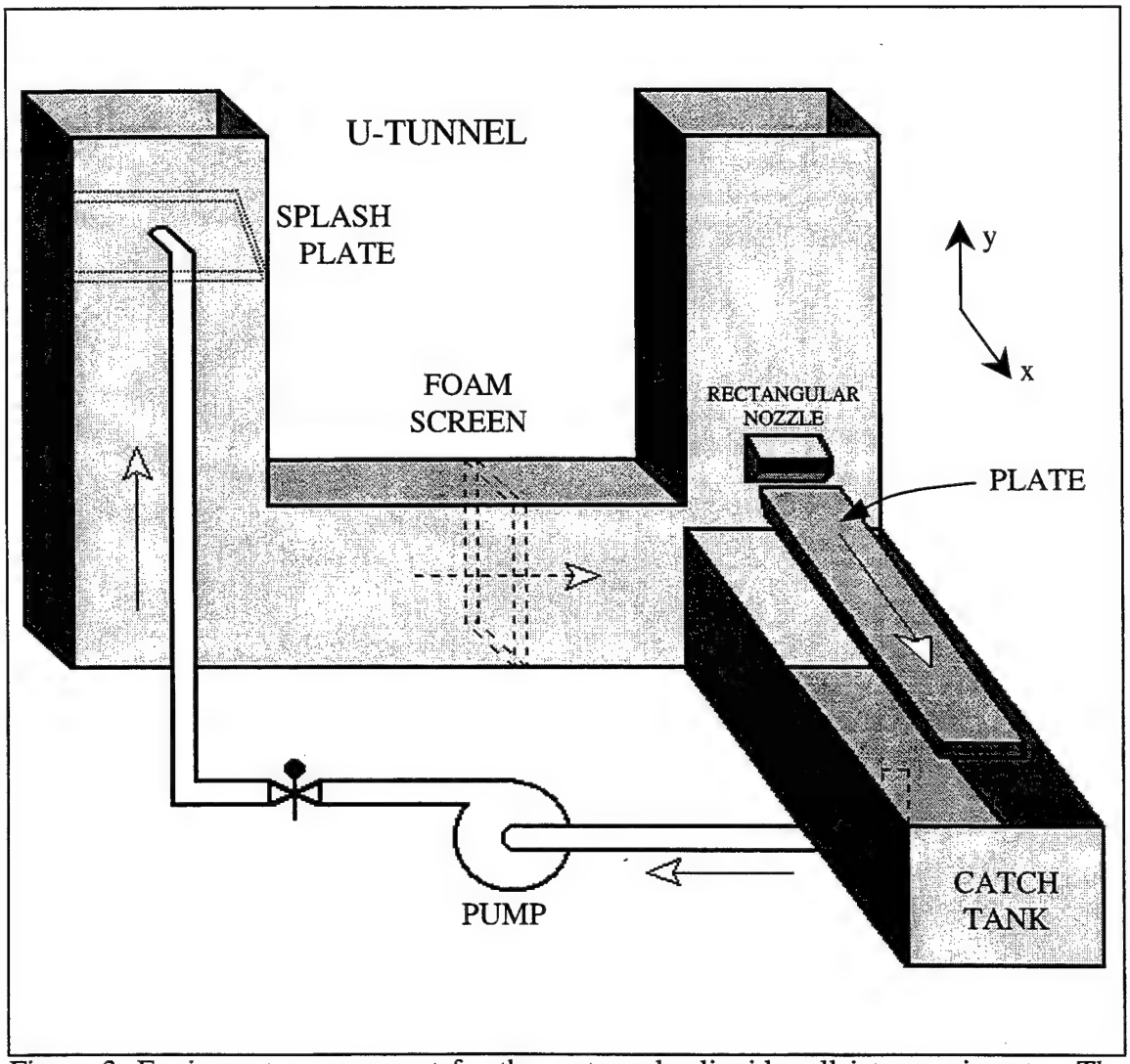

Figure 3. Equipment arrangement for the rectangular liquid wall jet experiments. The fluid flow path is as indicated by the arrows.

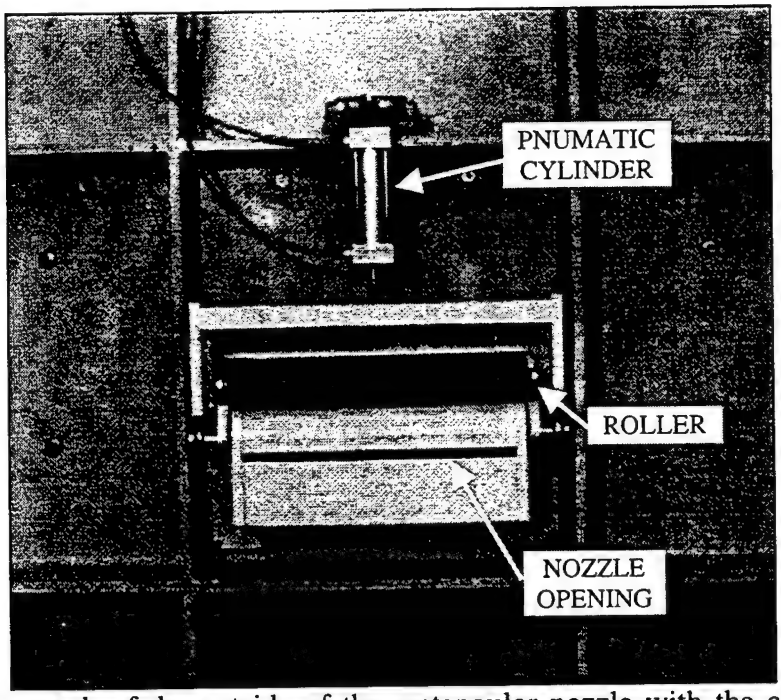

Figure 4. Photograph of the outside of the rectangular nozzle with the cylindrical gate open.

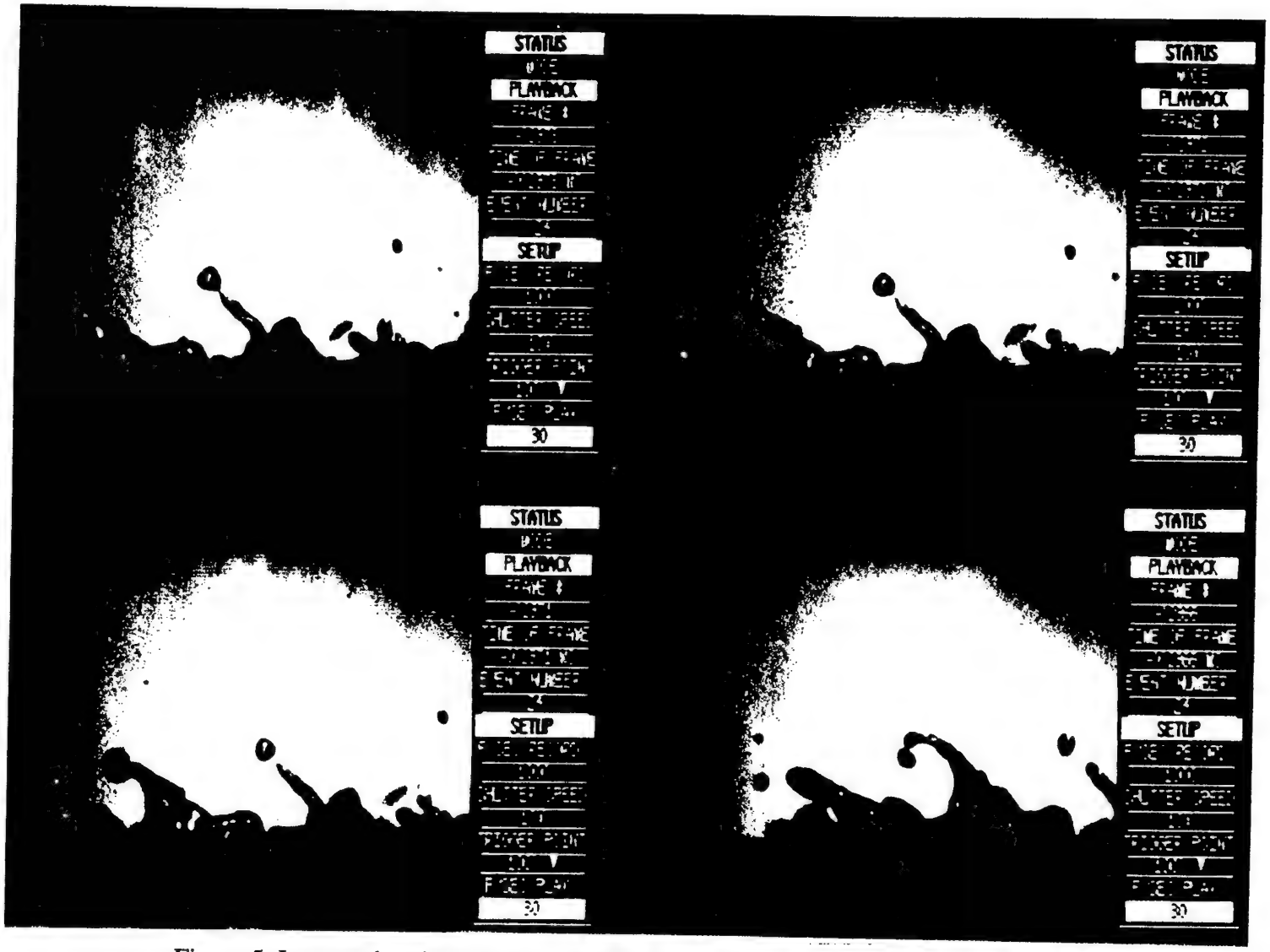

Figure 5. Images showing filament necking and subsequent drop formation.

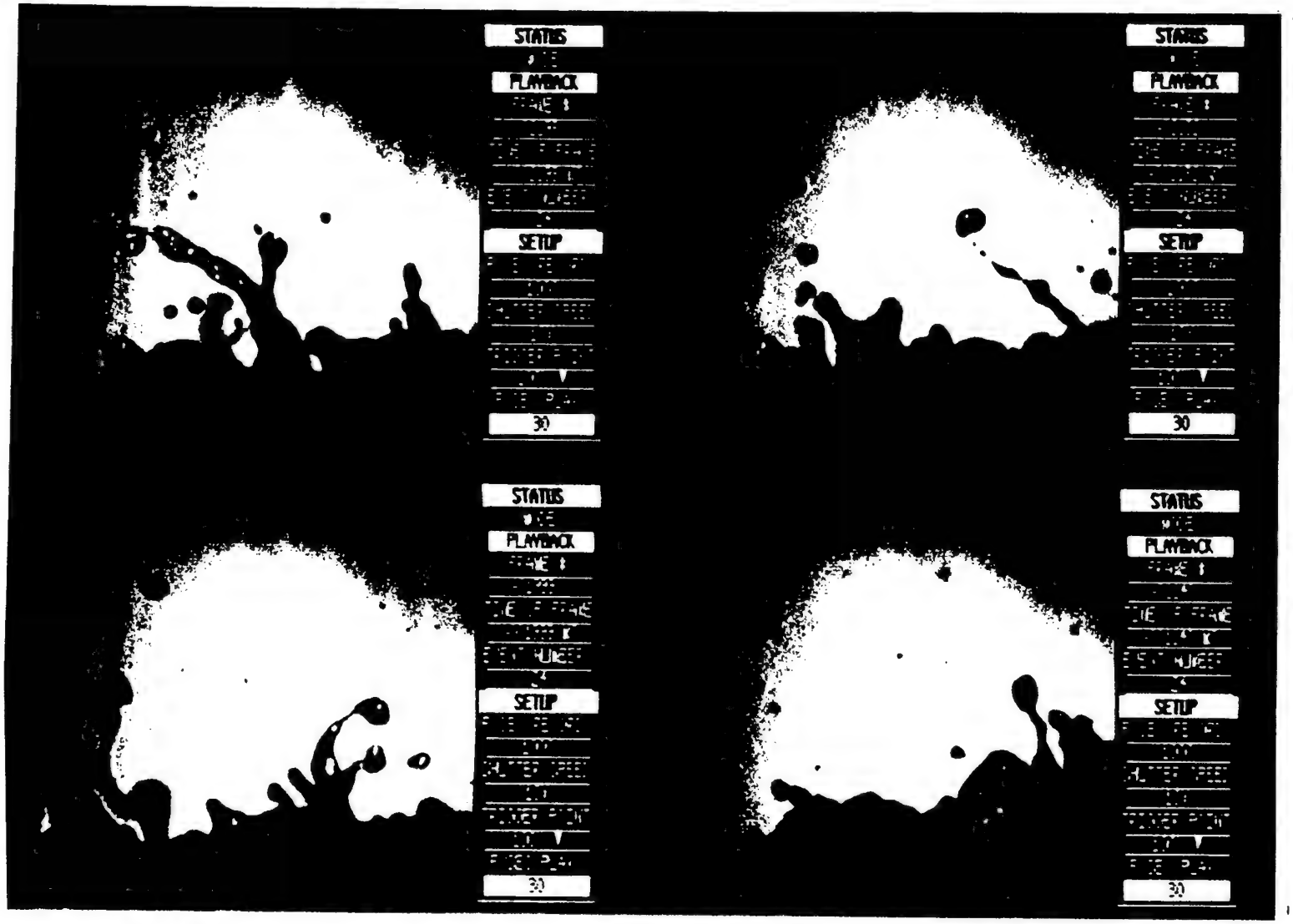

Figure 6. Image displaying multitude of filament and drop characteristics.

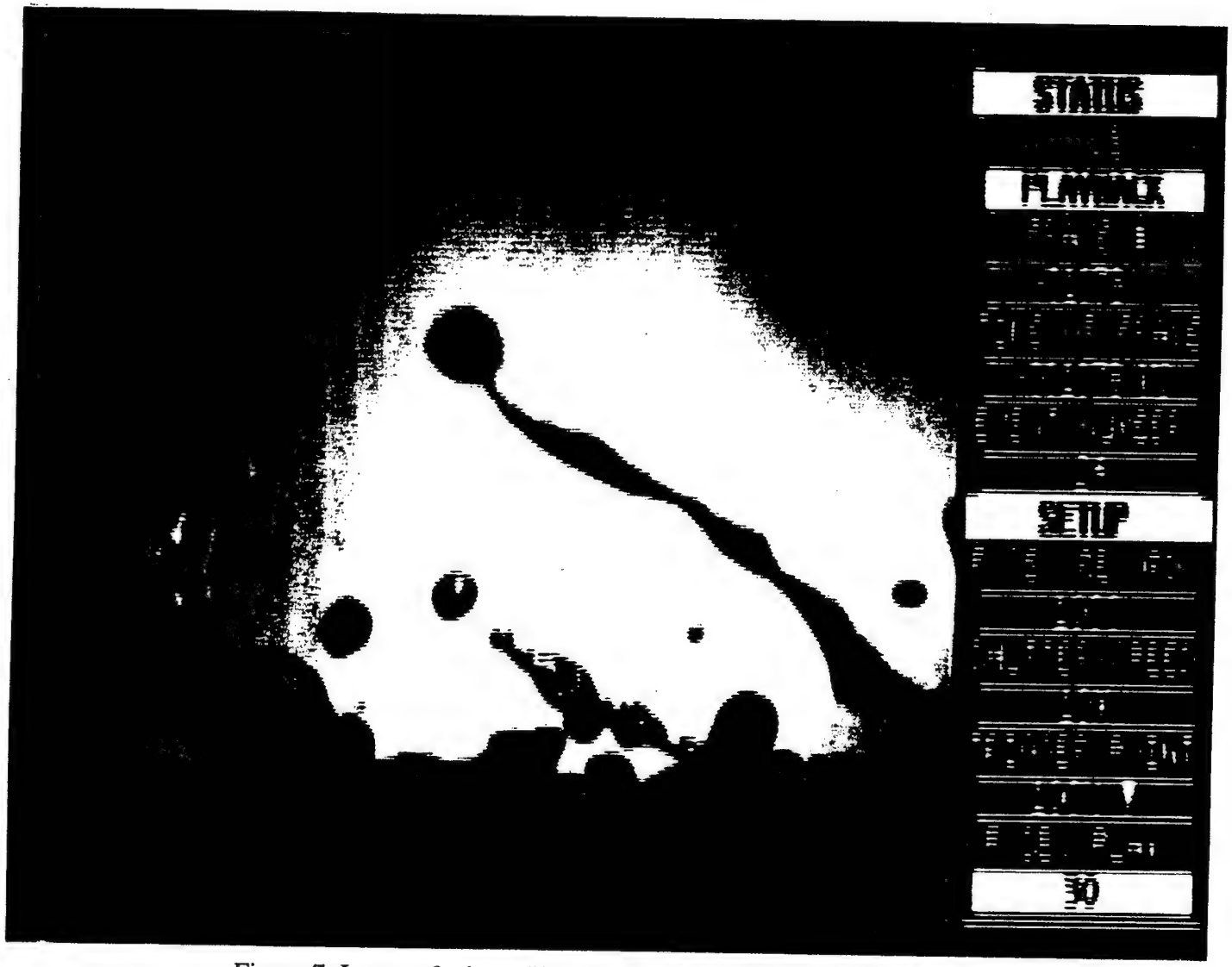

Figure 7. Image of a long filament with multiple neck regions.

Figure 8. Image of a filament just prior to drop formation.

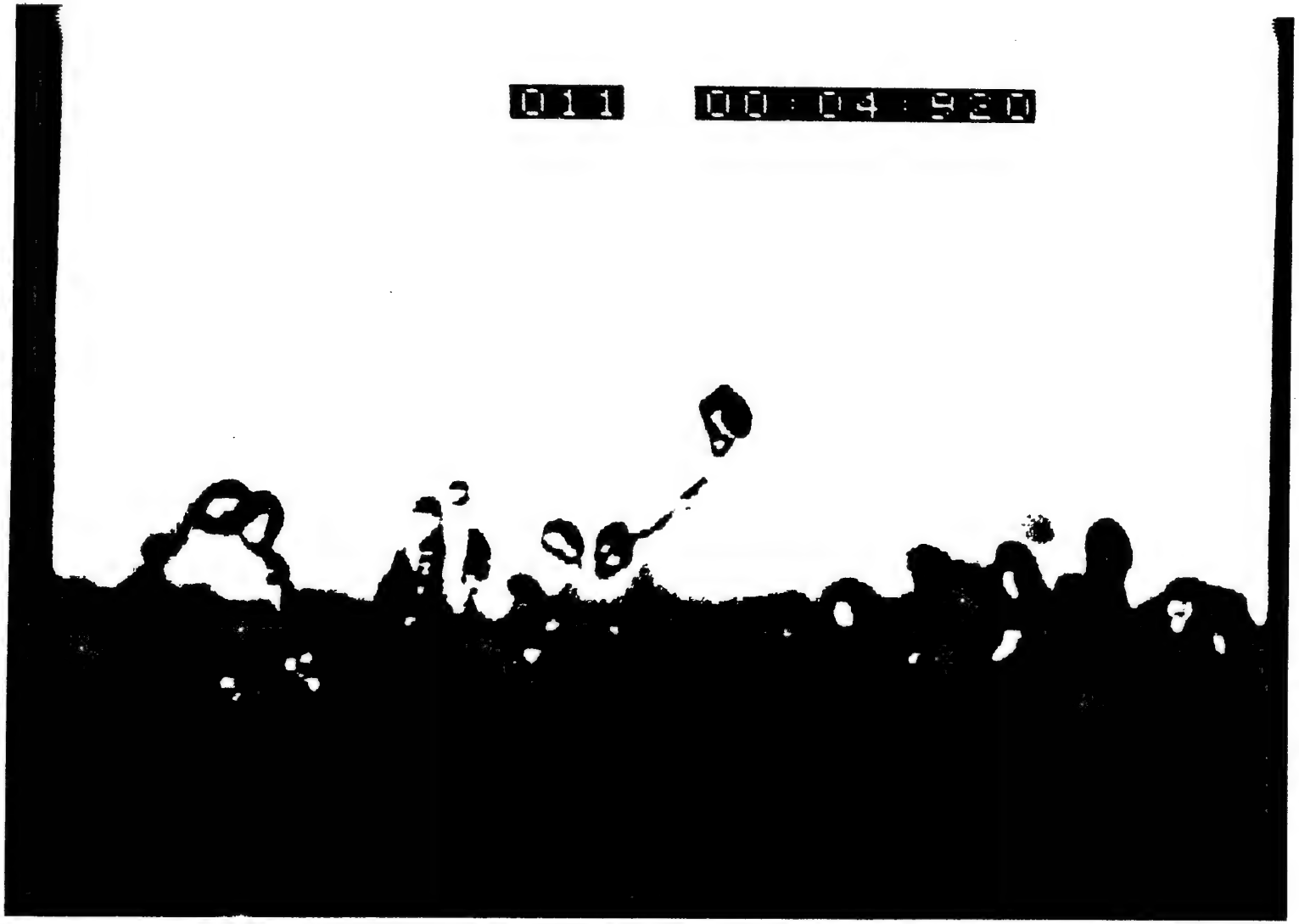

Figure 9. Image of filament that has detached from the free surface.

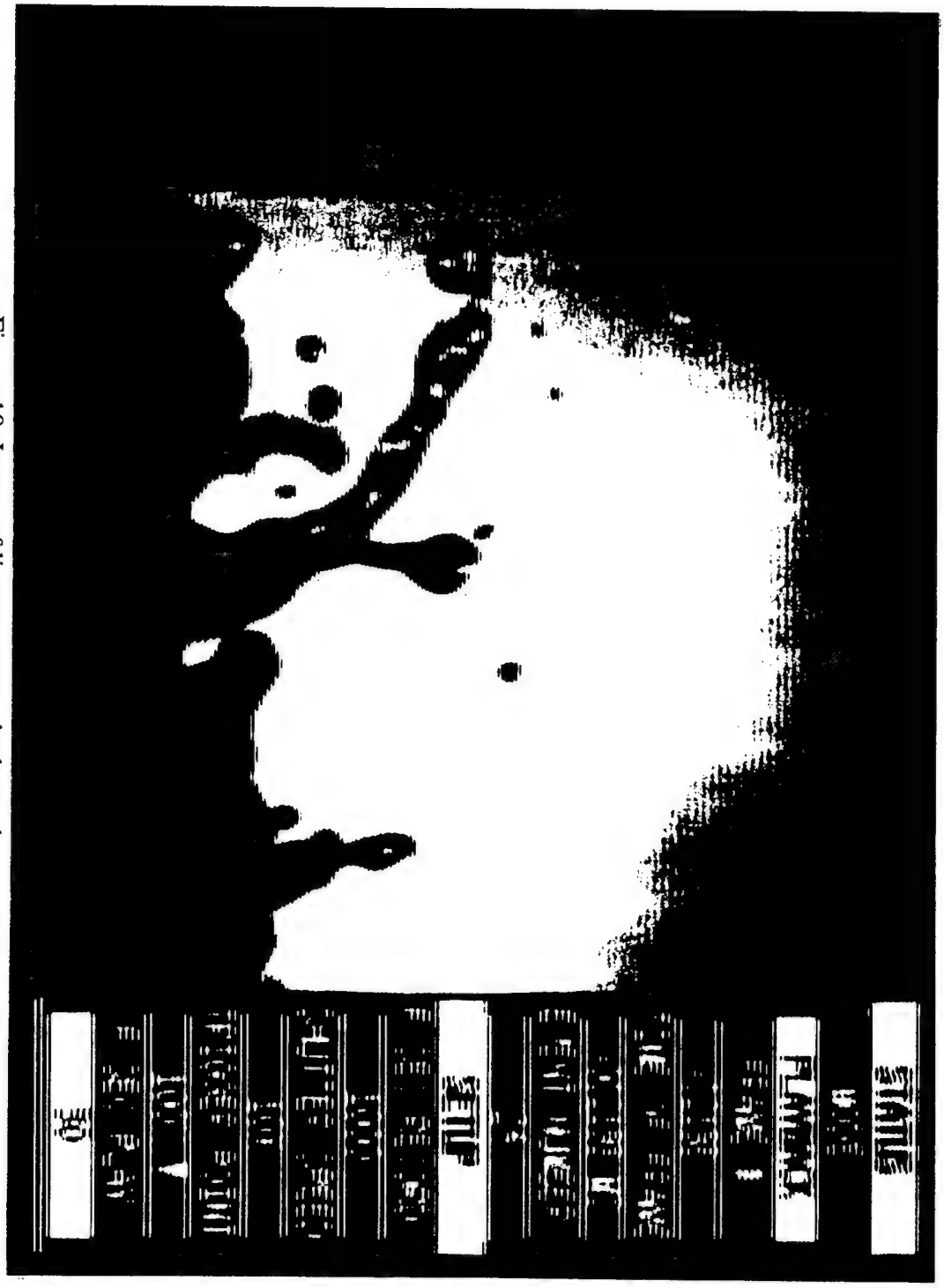

Figure 10. Image of ligaments attached together.

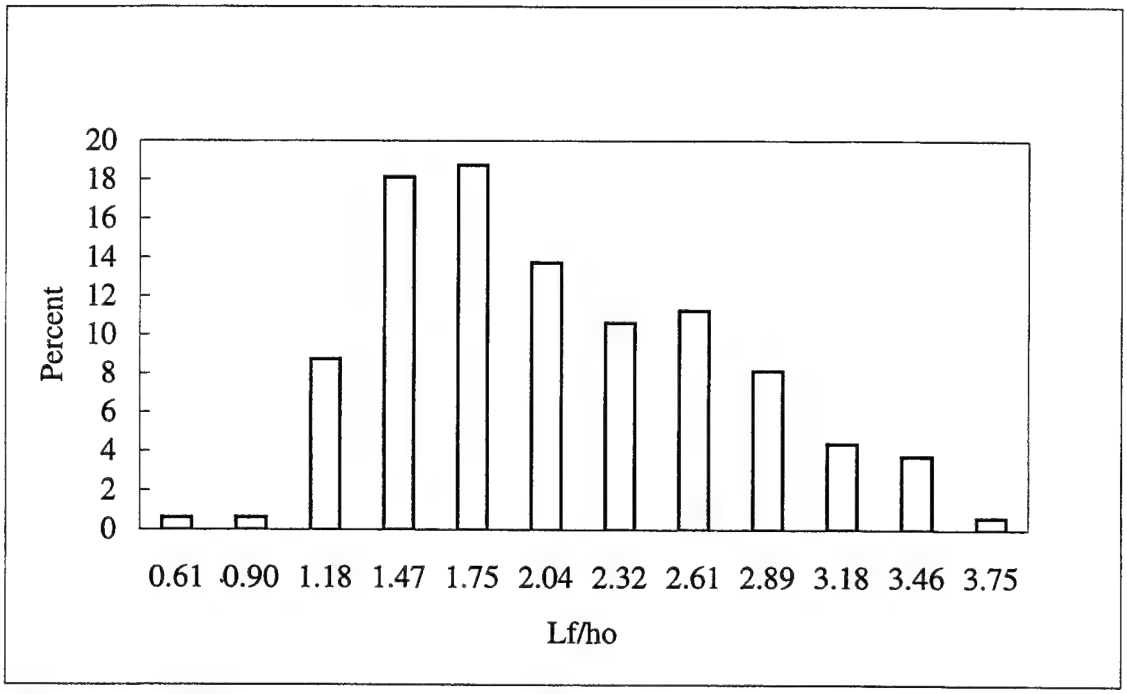

Figure 11. Distribution of the normalized filament length for fresh water half-free with jet thickness = 5.8 mm (k/ho = 0.06, We = 3014, Fr = 25.8).

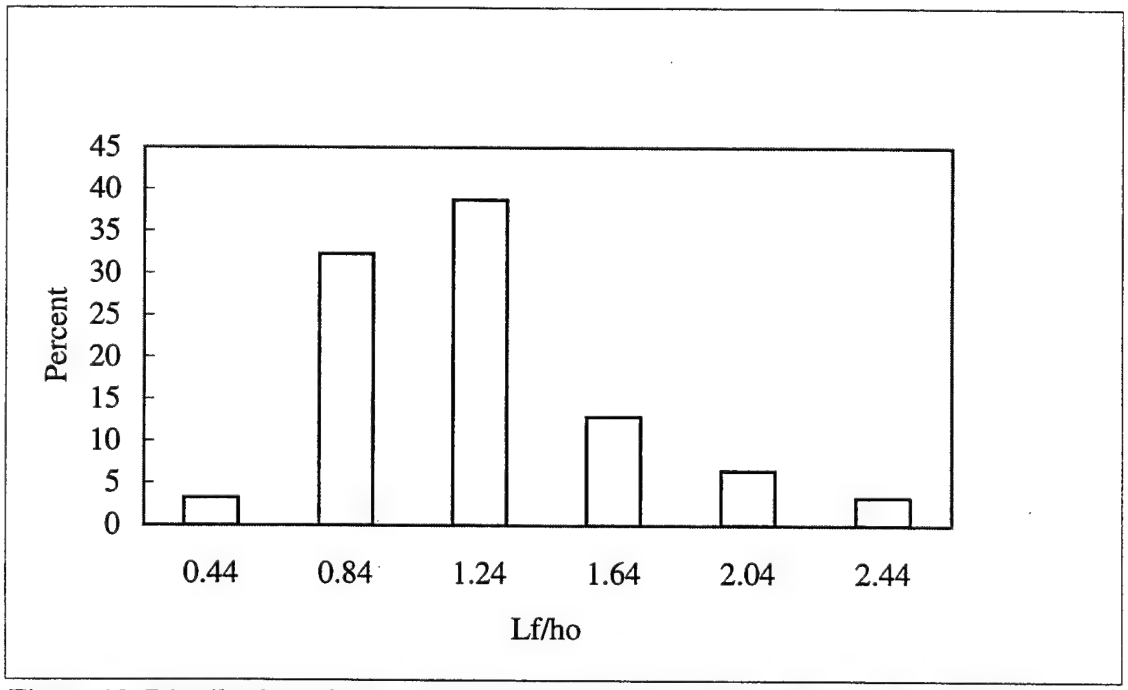

Figure 12. Distribution of the normalized filament length for fresh water half-free with jet thickness = 14.0 mm (k/ho = 0.06, We = 7367, Fr = 16.6).

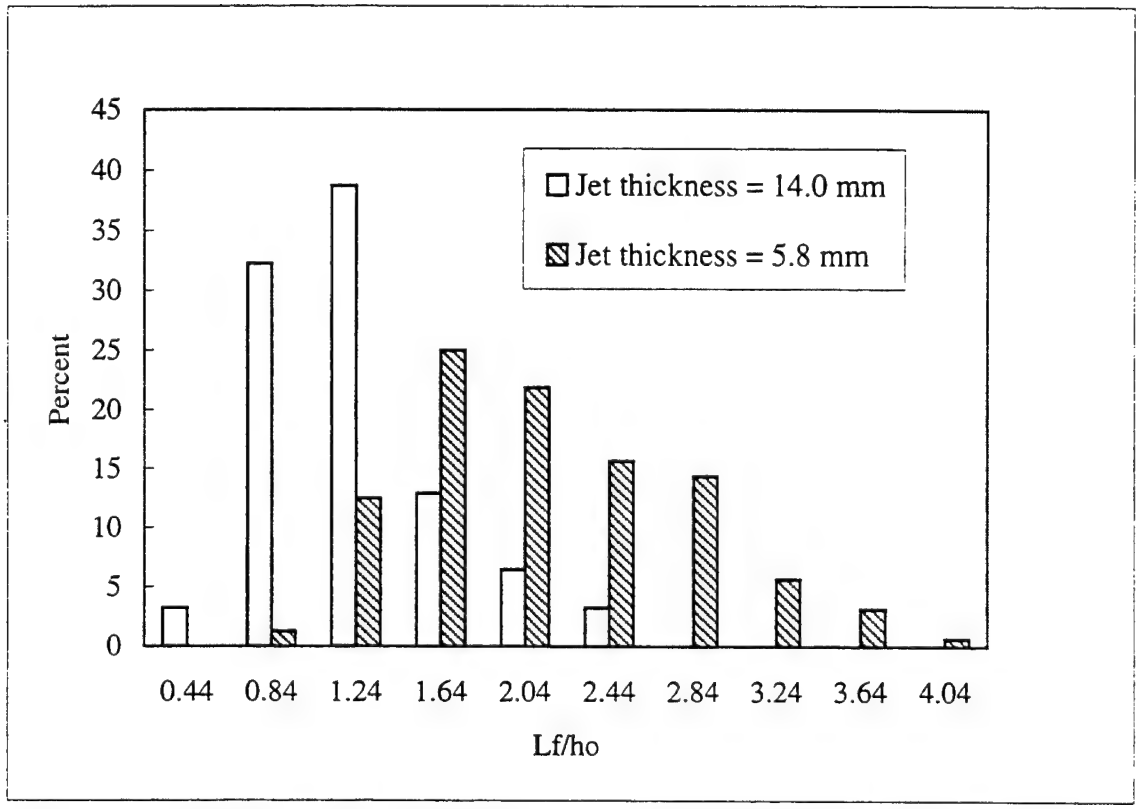

Figure 13. Comparison of the distributions of normalized filament length for fresh water half-free jet for two jet thicknesses.

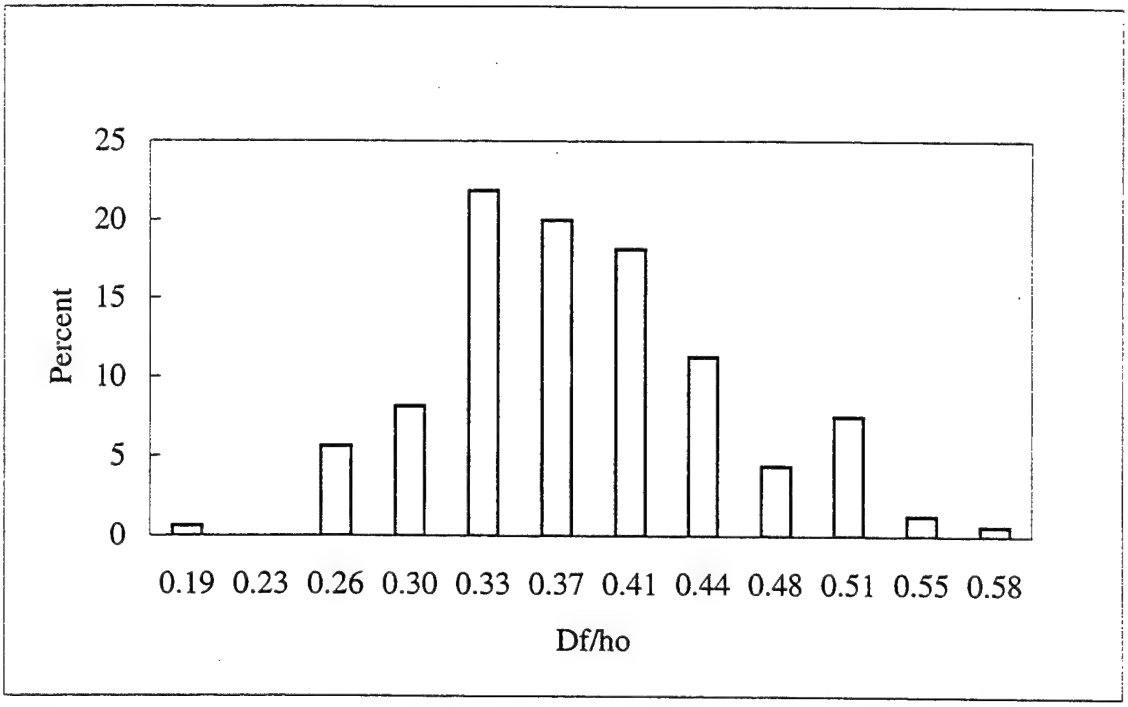

Figure 14. Distribution of normalized filament diameter for fresh water half-free jet with jet thickness = 5.8 mm (k/ho = 0.06, We = 3014, Fr = 25.8).

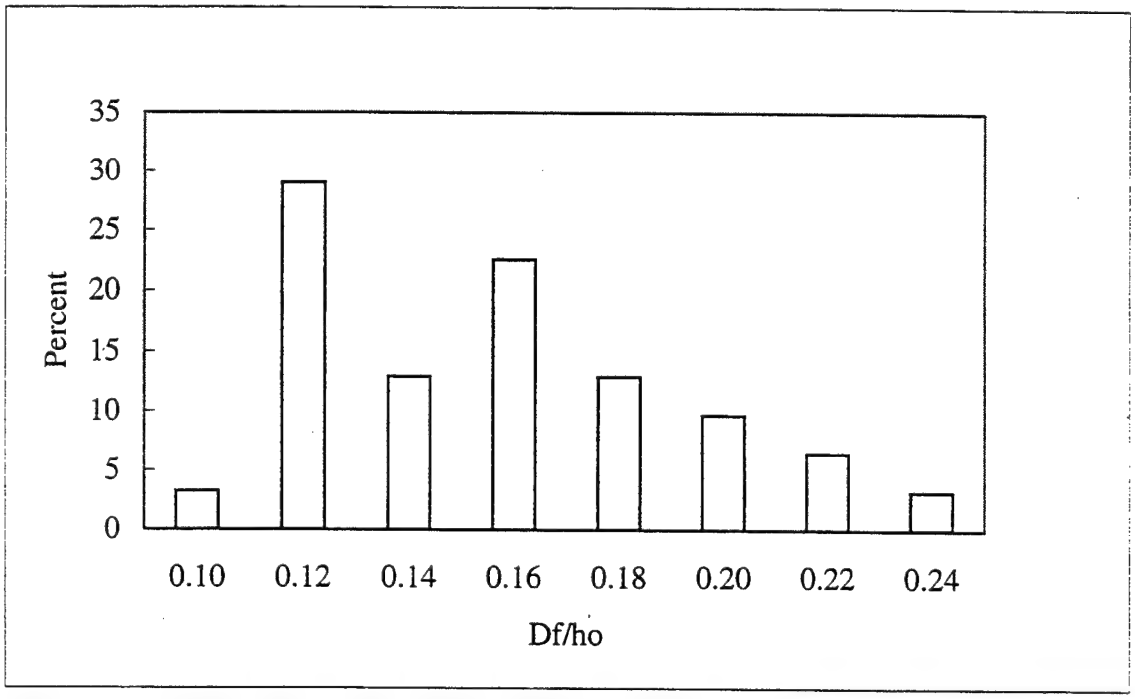

Figure 15. Distribution of normalized filament diameter for fresh water half-free jet with jet thickness = 14.0 mm (k/ho = 0.06, We = 7367, Fr = 16.6).

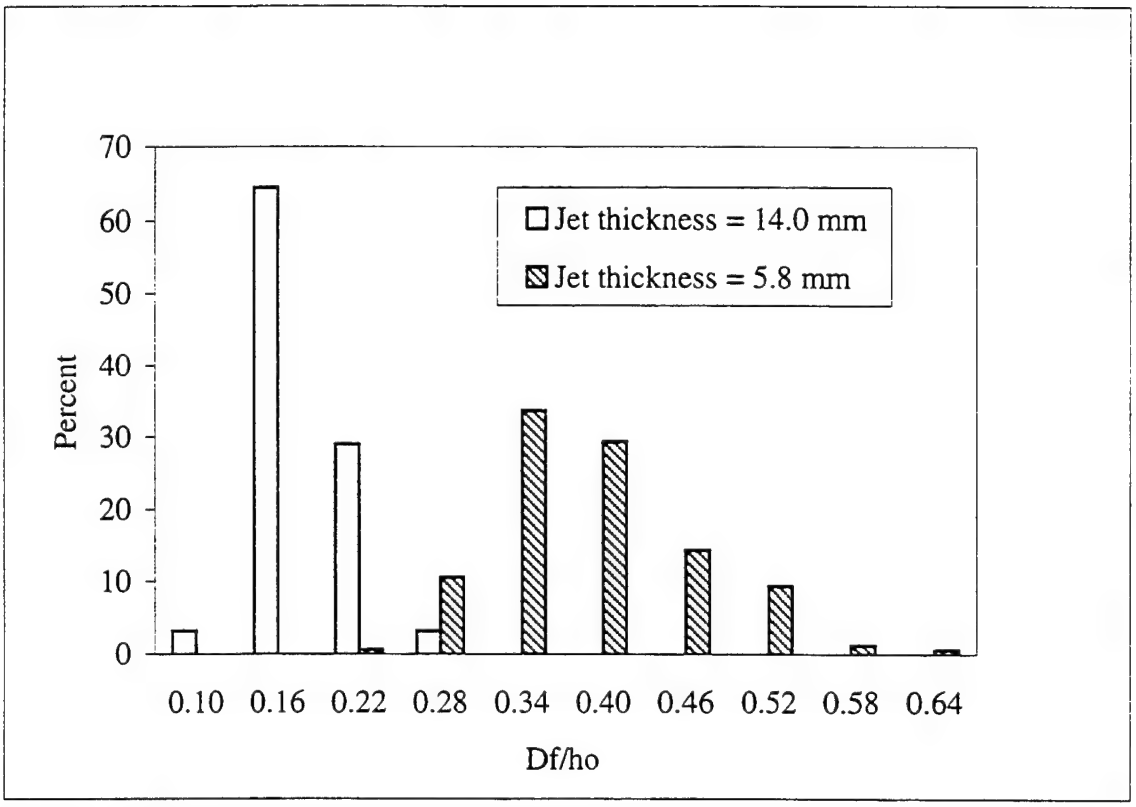

Figure 16. Comparison of the distributions of normalized filament diameter for fresh water half-free jet for two jet thicknesses.

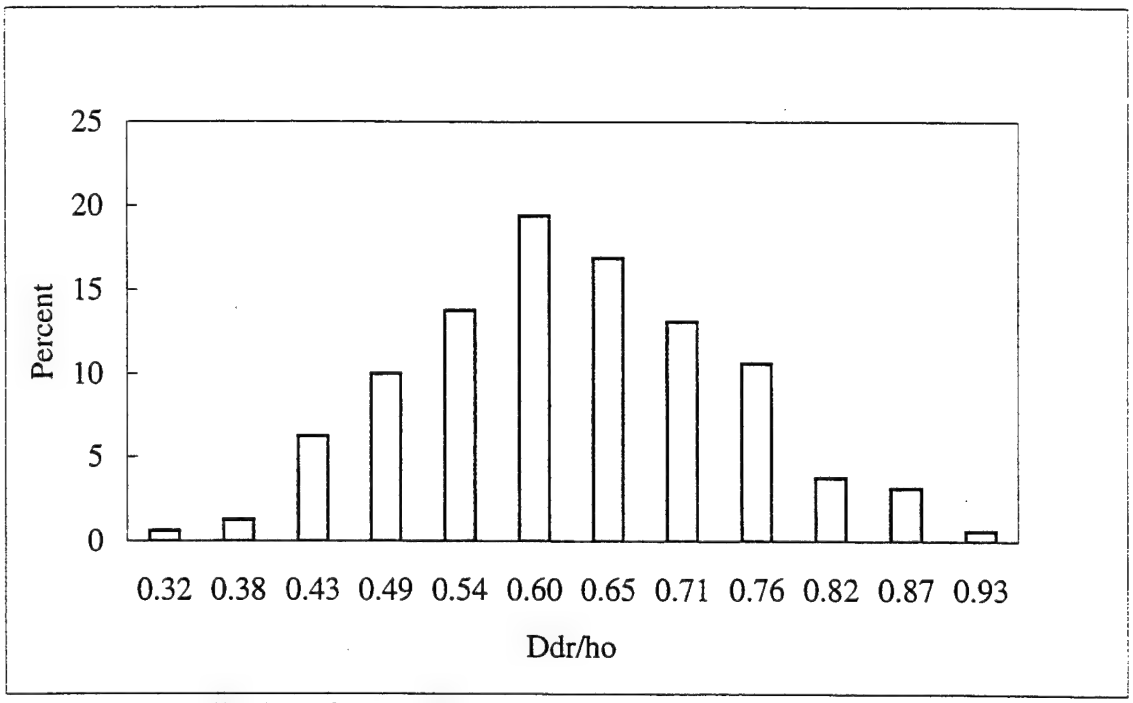

Figure 17. Distribution of normalized drop diameter for fresh water half-free jet with jet thickness = 5.8 mm (k/ho = 0.06, We = 3014, Fr = 25.8).

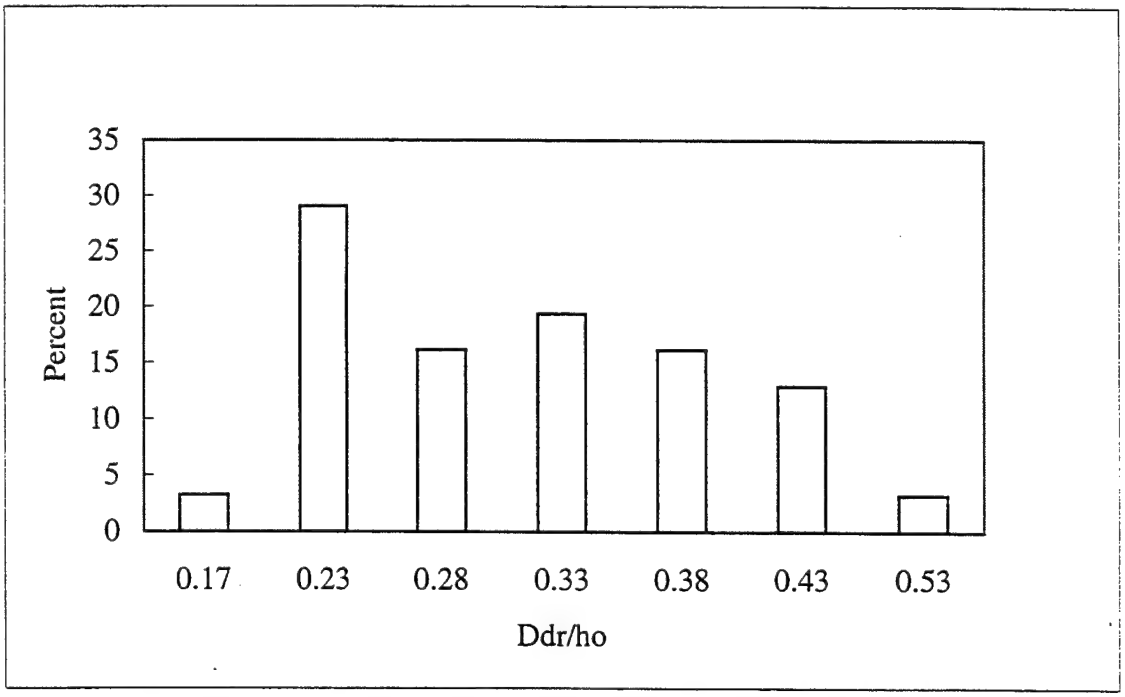

Figure 18. Distribution of normalized drop diameter for fresh water half-free jet with jet thickness = 14.0 mm (k/ho = 0.06, We = 7367, Fr = 16.6).

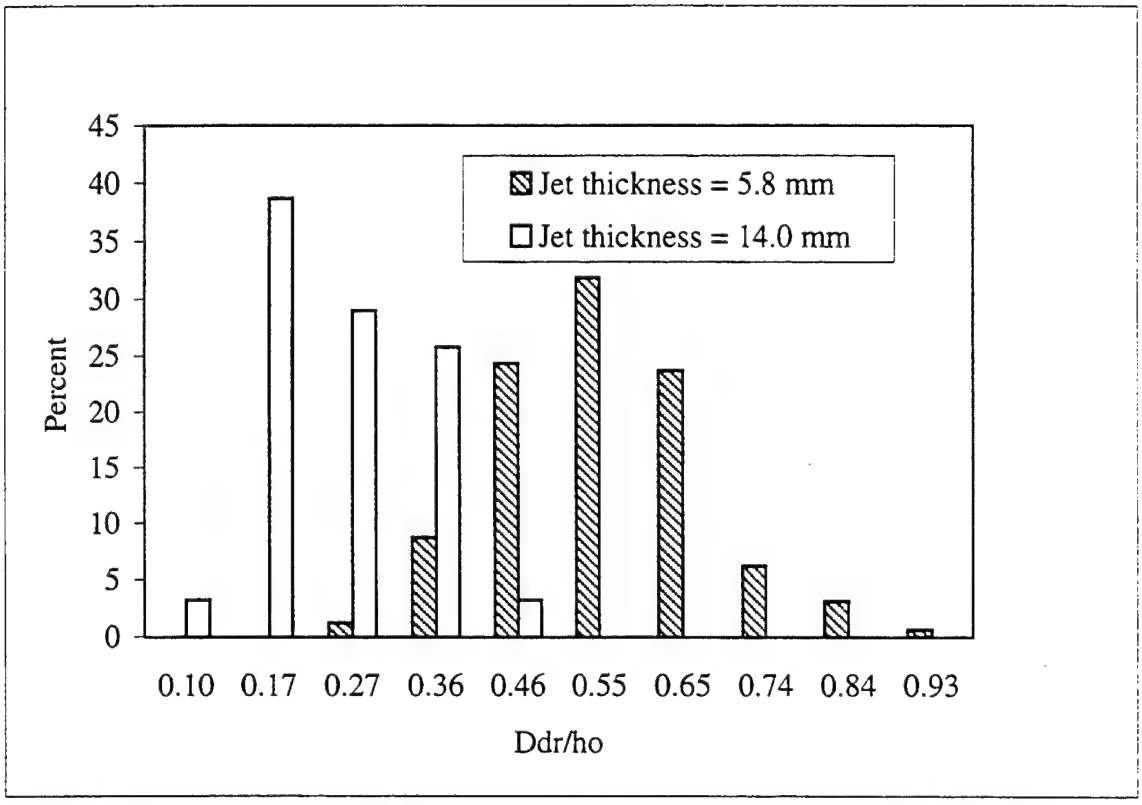

Figure 19. Comparison of the distributions of normalized drop diameter for fresh water half-free jet for two jet thicknesses.

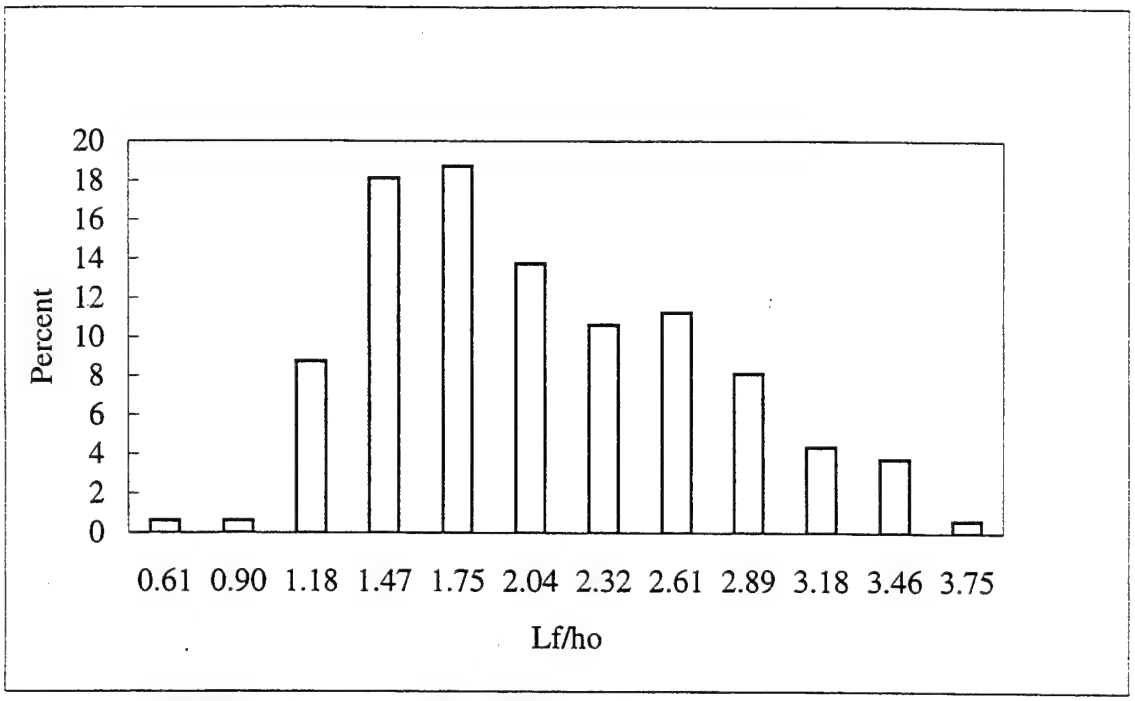

Figure 20. Distribution of normalized filament length for fresh water half-free jet (k/ho = 0.06, We = 3014, Fr = 25.8, ho = 5.8 mm).

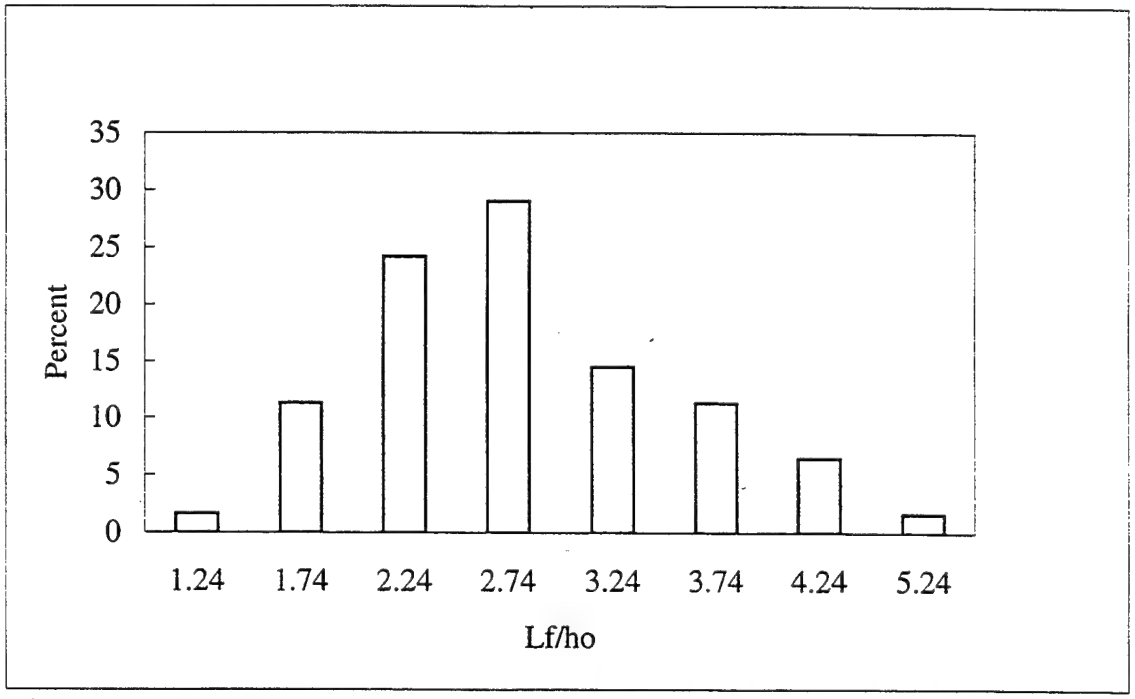

Figure 21. Distribution of normalized filament length for salt water half-free jet (k/ho = 0.06, We = 3095, Fr = 25.8, ho = 5.8 mm).

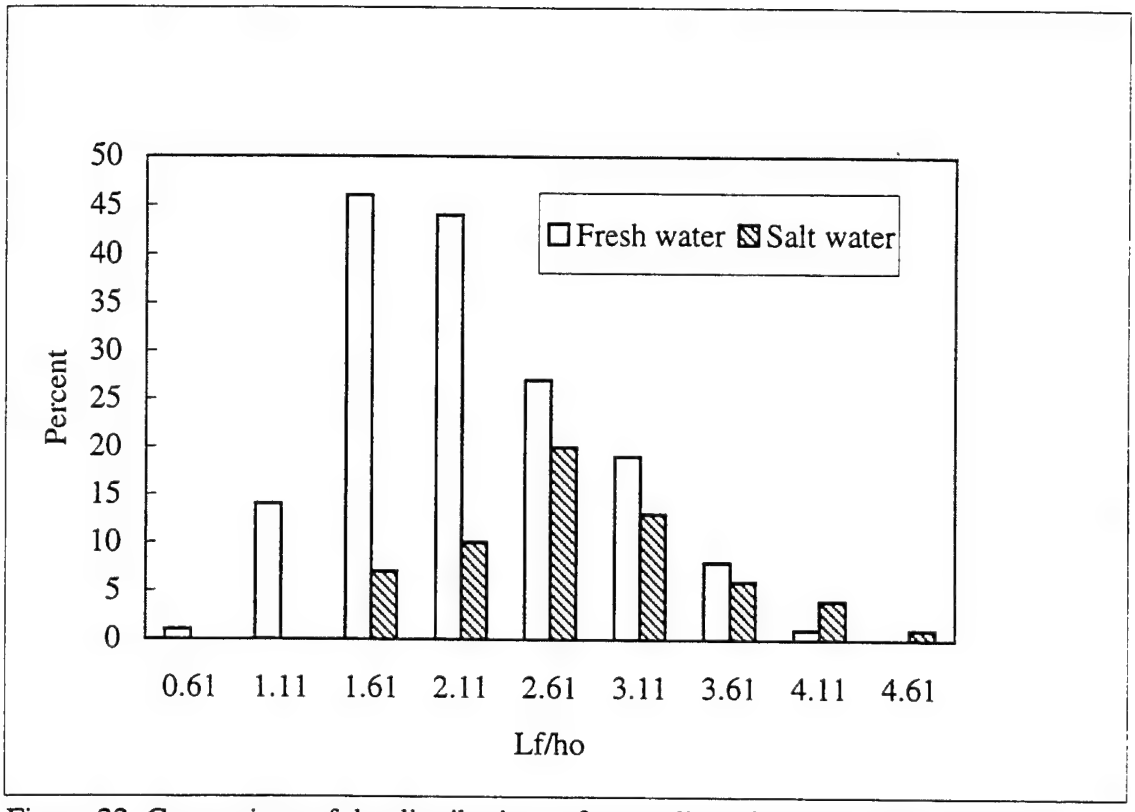

Figure 22. Comparison of the distributions of normalized filament length for fresh and salt water half-free jets.

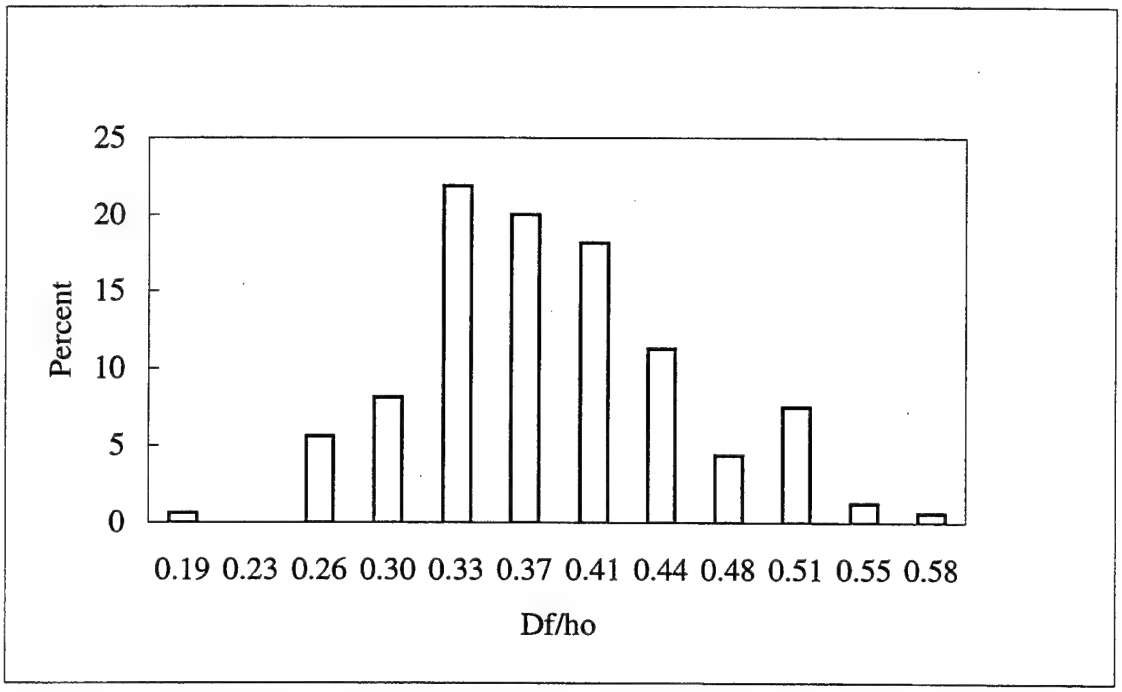

Figure 23. Distribution of normalized filament diameter for fresh water half-free jet (k/ho = 0.06, We = 3014, Fr = 25.8, ho = 5.8 mm).

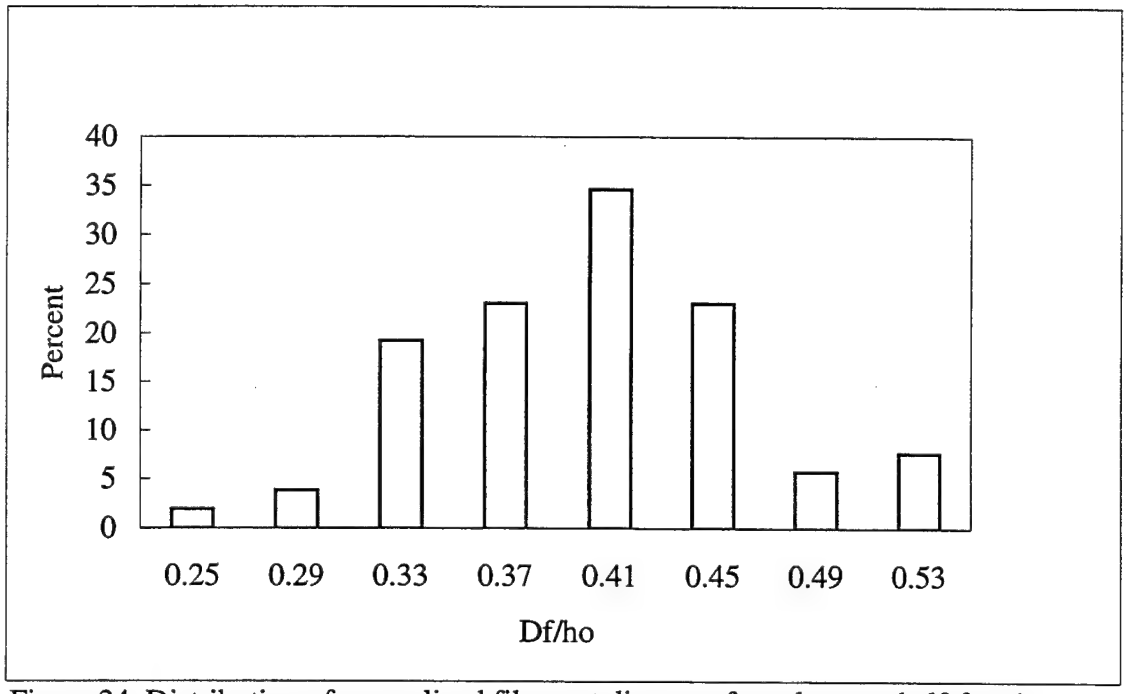

Figure 24. Distribution of normalized filament diameter for salt water half-free jet (k/ho = 0.06, We = 3095, Fr = 25.8, ho = 5.8 mm).

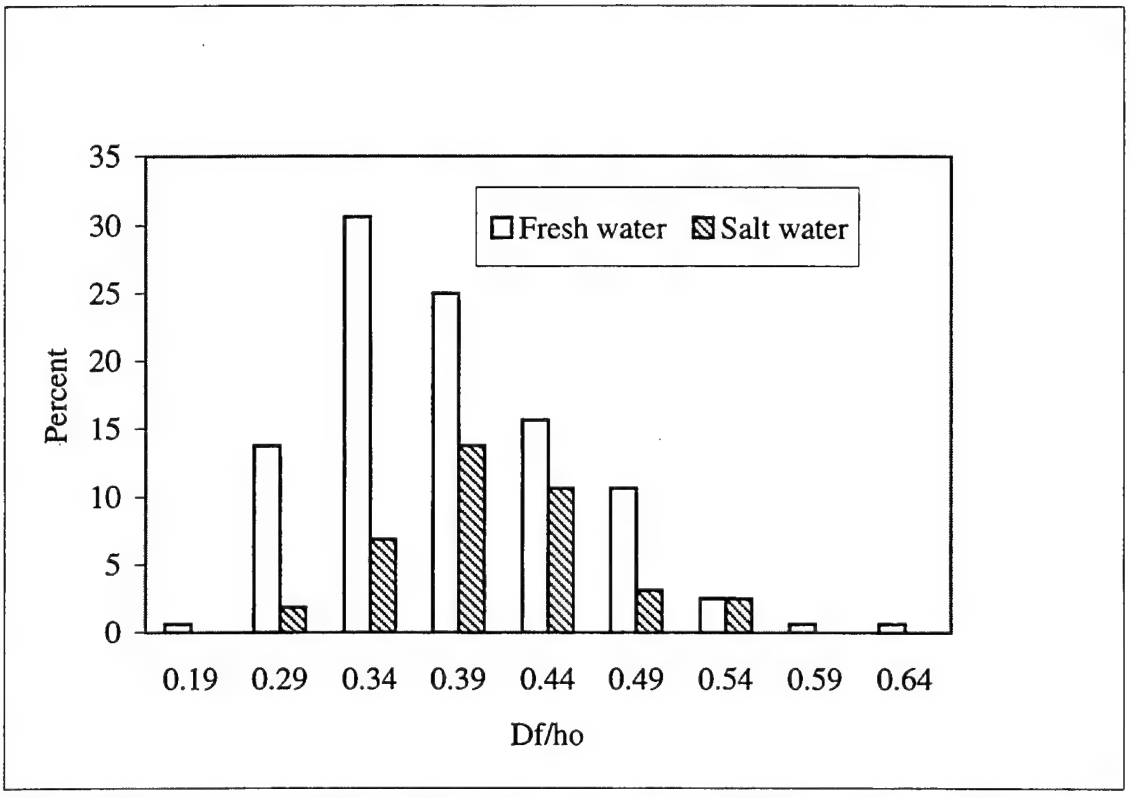

Figure 25. Comparison of the distributions of normalized filament diameter for fresh and salt water half-free jets.

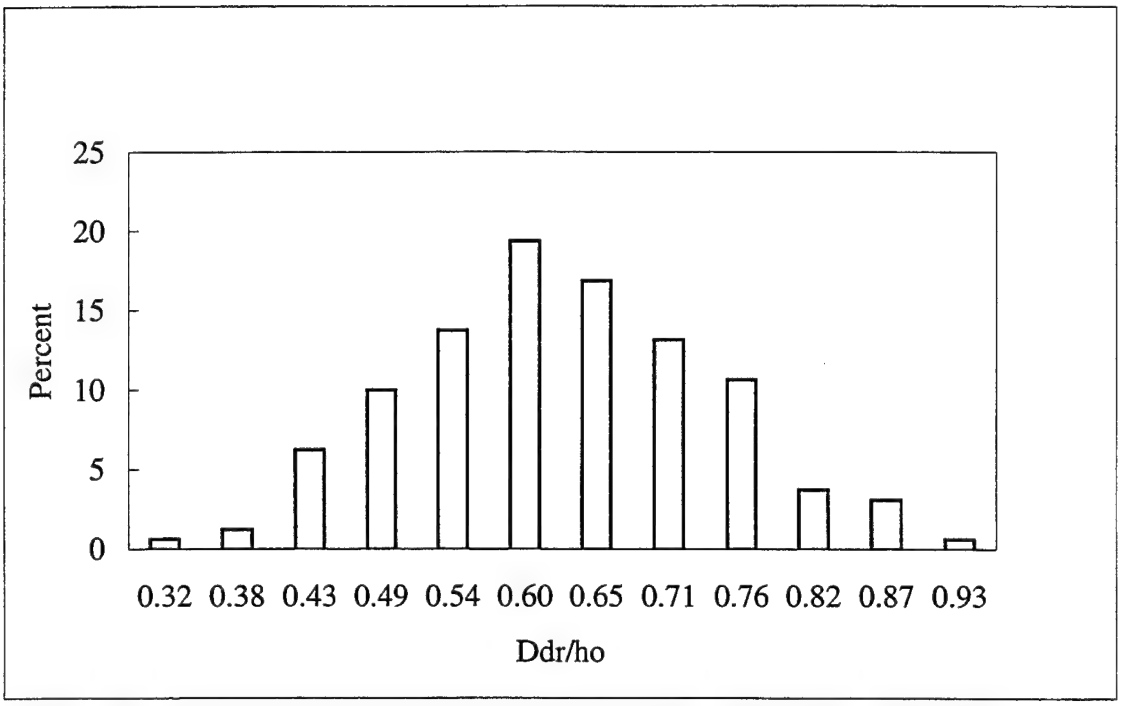

Figure 26. Distribution of normalized drop diameter for fresh water half-free jet k/ho = 0.06, We = 3014, Fr = 25.8, ho = 5.8 mm).

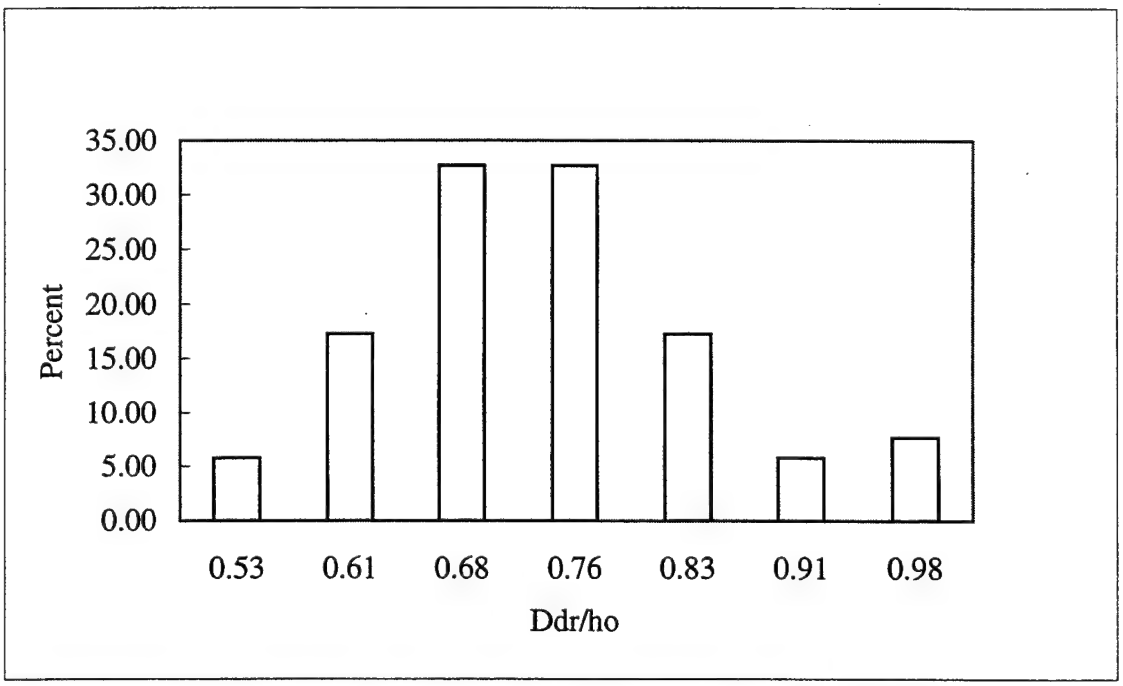

Figure 27. Distribution of normalized drop diameter for salt water half-free jet k/ho = 0.06, We = 3095, Fr = 25.8, ho = 5.8 mm).

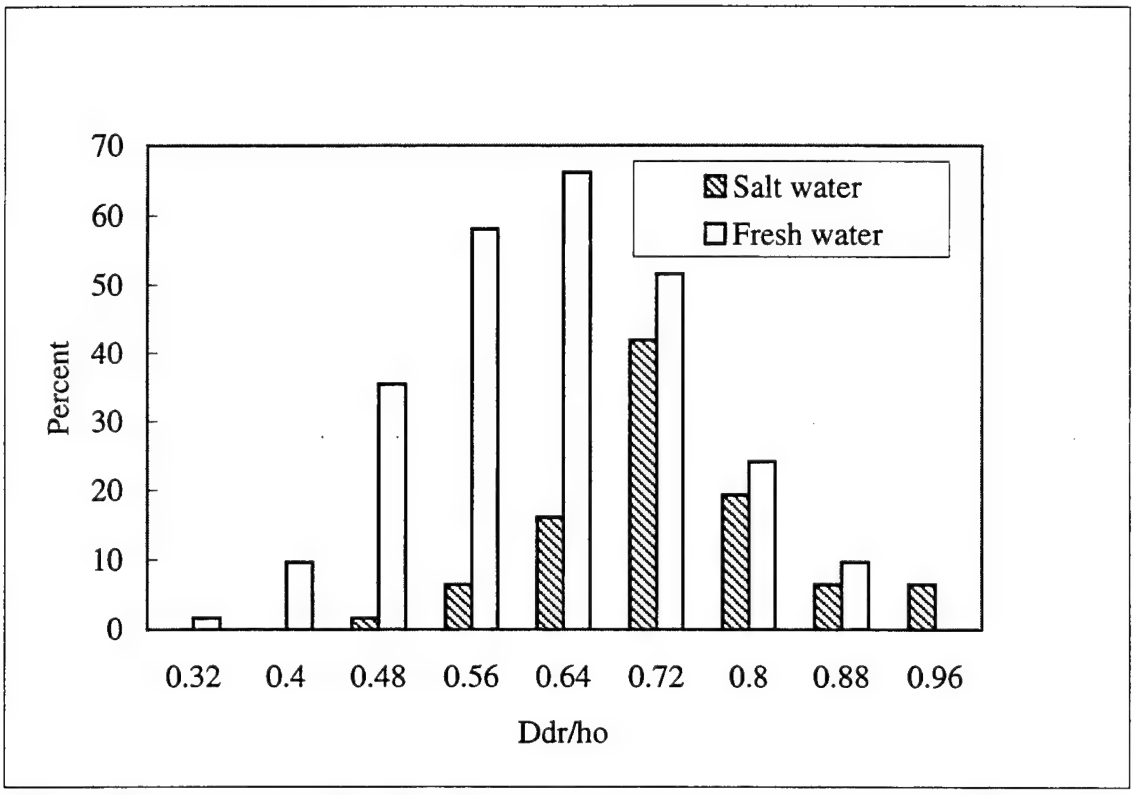

Figure 28. Comparison of the distributions of normalized drop diameter for fresh and salt water half-free jets.

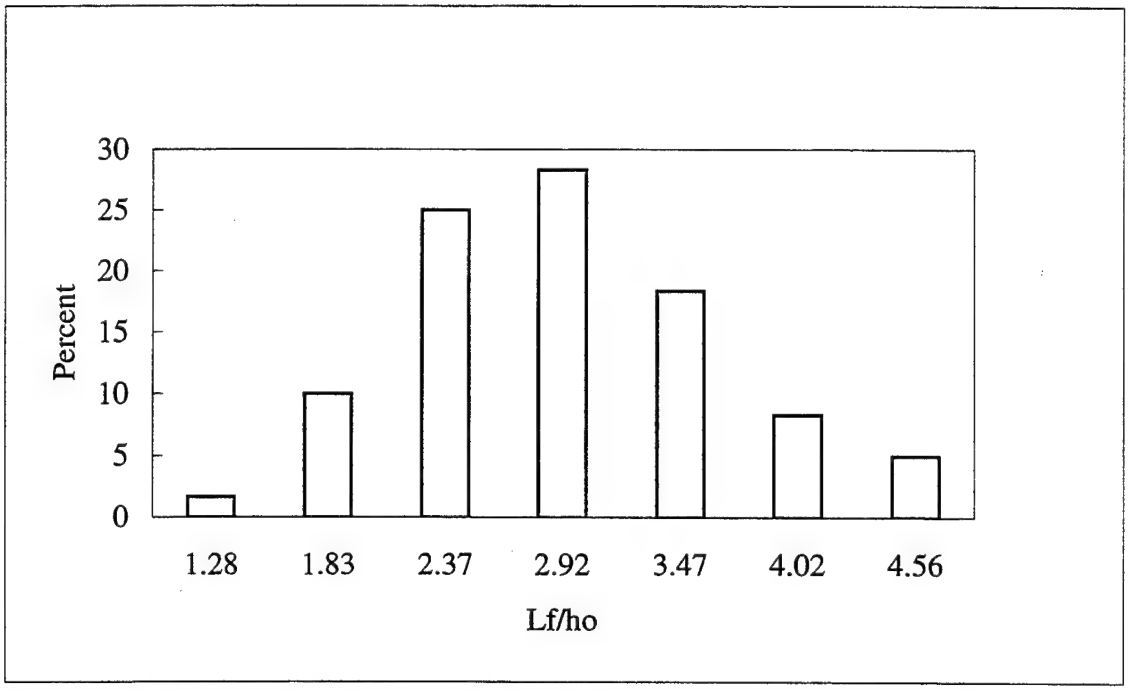

Figure 29. Distribution of normalized filament length for salt water free jet at 10 degree ramp angle (k/ho = 0.06, We = 3095, Fr = 25.8, ho = 5.8 mm).

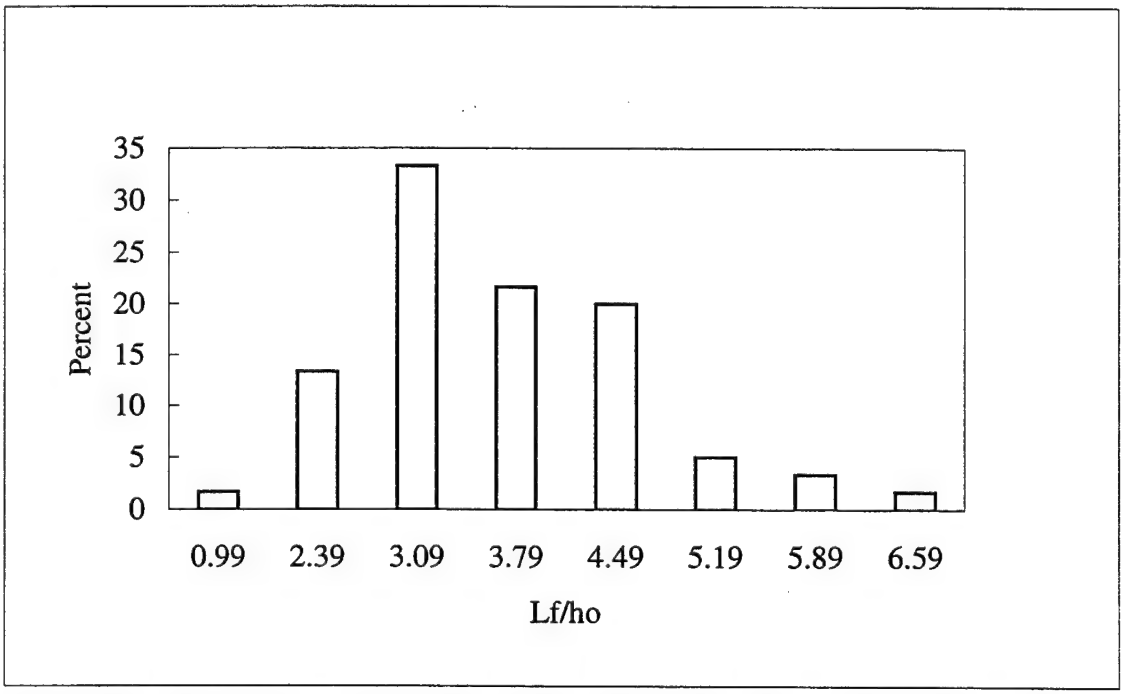

Figure 30. Distribution of normalized filament length for fresh water free jet at 10 degree ramp angle (k/ho = 0.06, We = 3014, Fr = 25.8, ho = 5.8 mm).

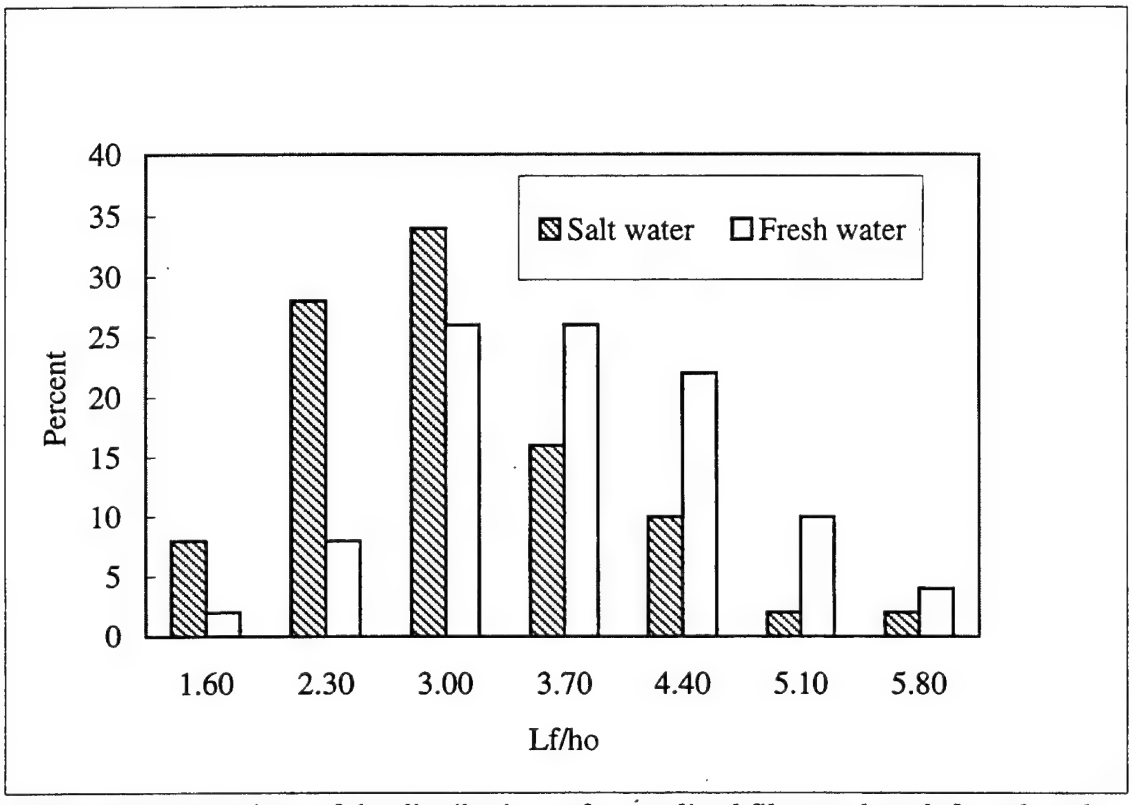

Figure 31. Comparison of the distributions of normalized filament length for salt and fresh water free jets at 10 degree ramp angle.

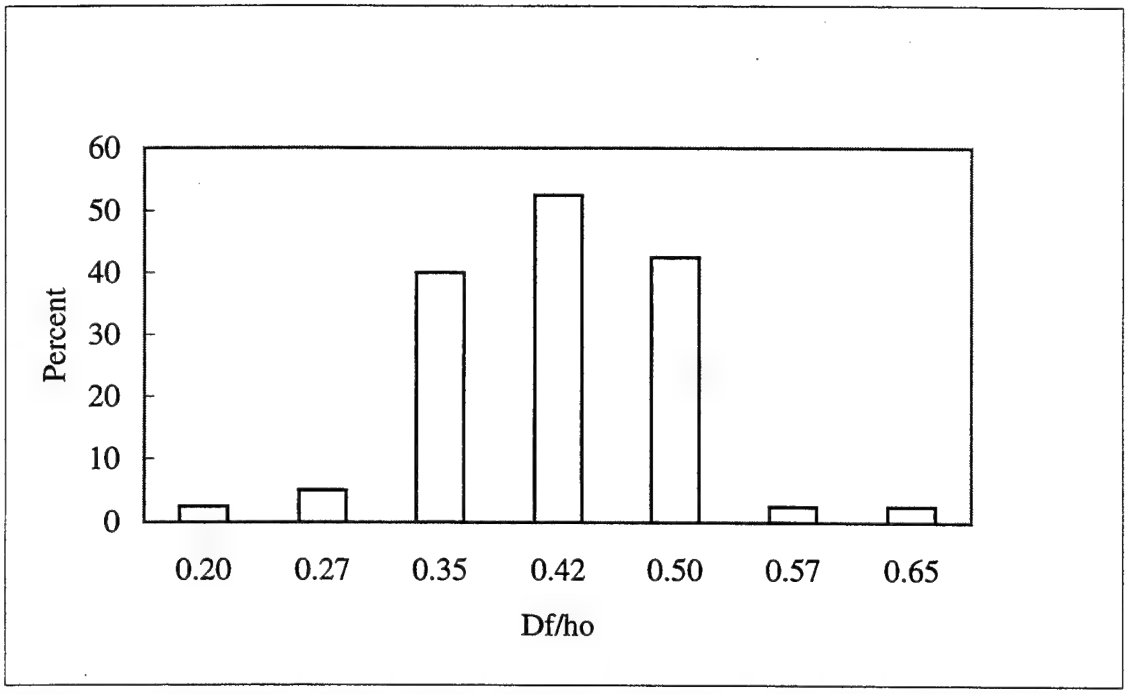

Figure 32. Distribution of normalized filament diameter for salt water free jet at 10 degree ramp angle (k/ho = 0.06, We = 3095, Fr = 25.8, ho = 5.8 mm).

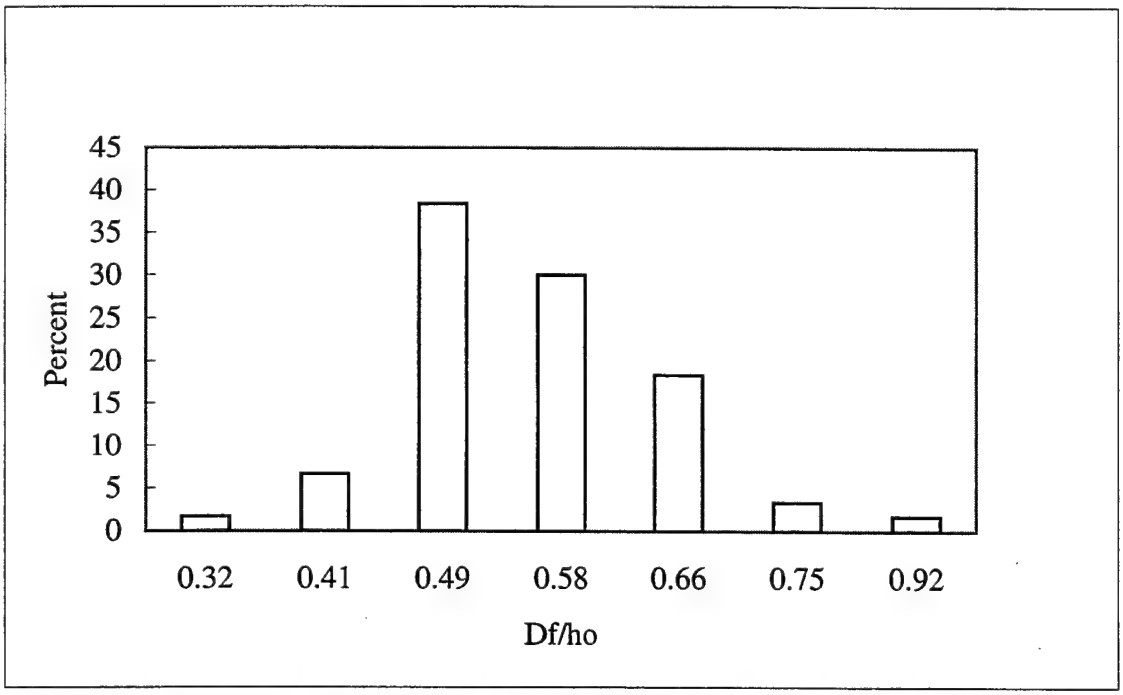

Figure 33. Distribution of normalized filament diameter for fresh water free jet at 10 degree ramp angle (k/ho = 0.06, We = 3014, Fr = 25.8, ho = 5.8 mm).

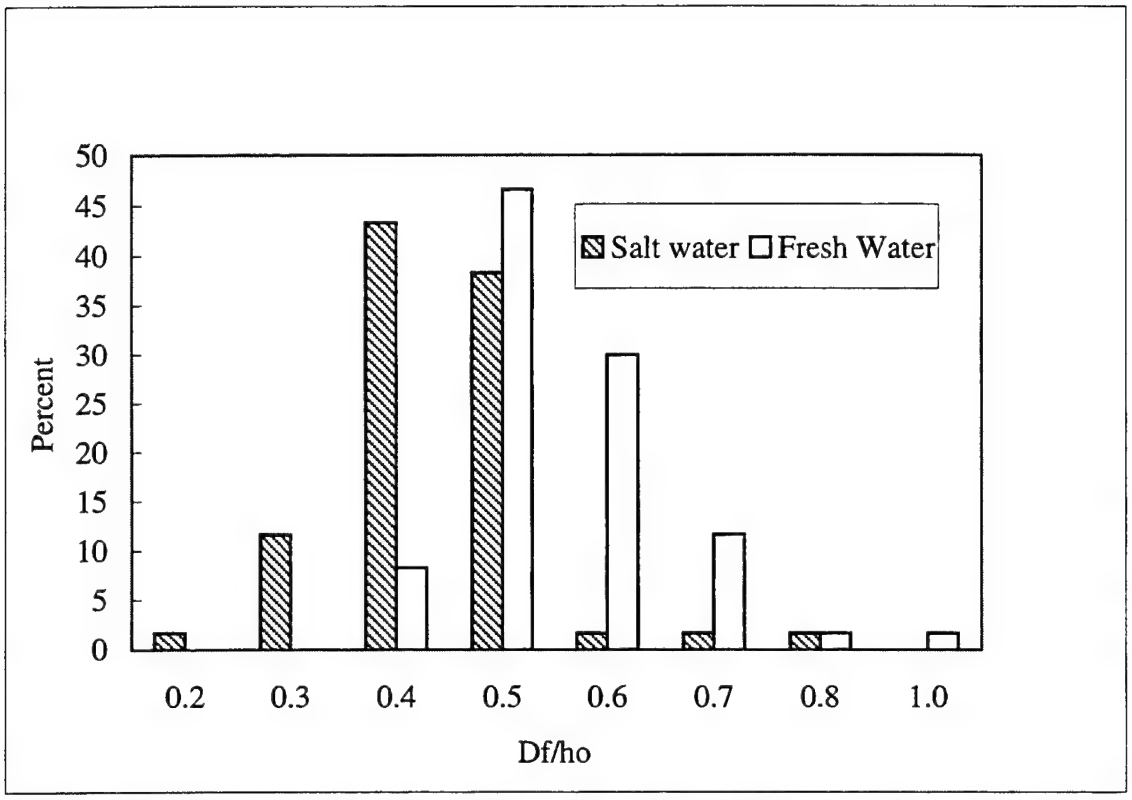

Figure 34. Comparison of the distributions of normalized filament diameter for salt and fresh water free jets at 10 degree ramp angle.

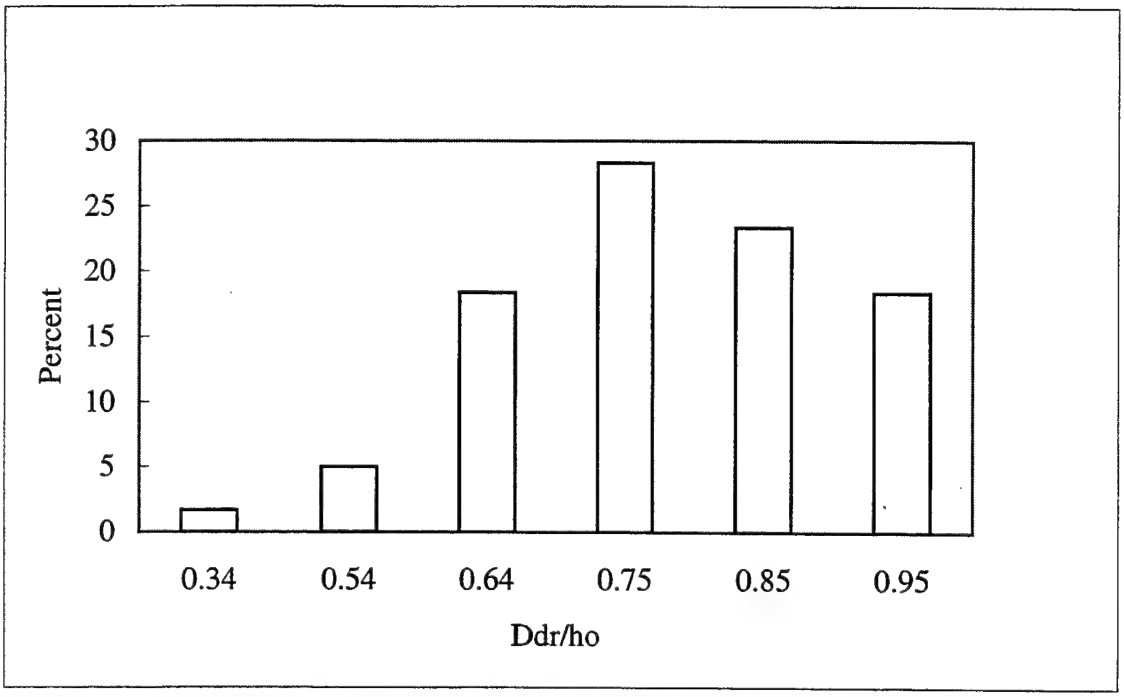

Figure 35. Distribution of normalized drop diameter for salt water free jet at 10 degree ramp angle (k/ho = 0.06, We = 3095, Fr = 25.8, ho = 5.8 mm).

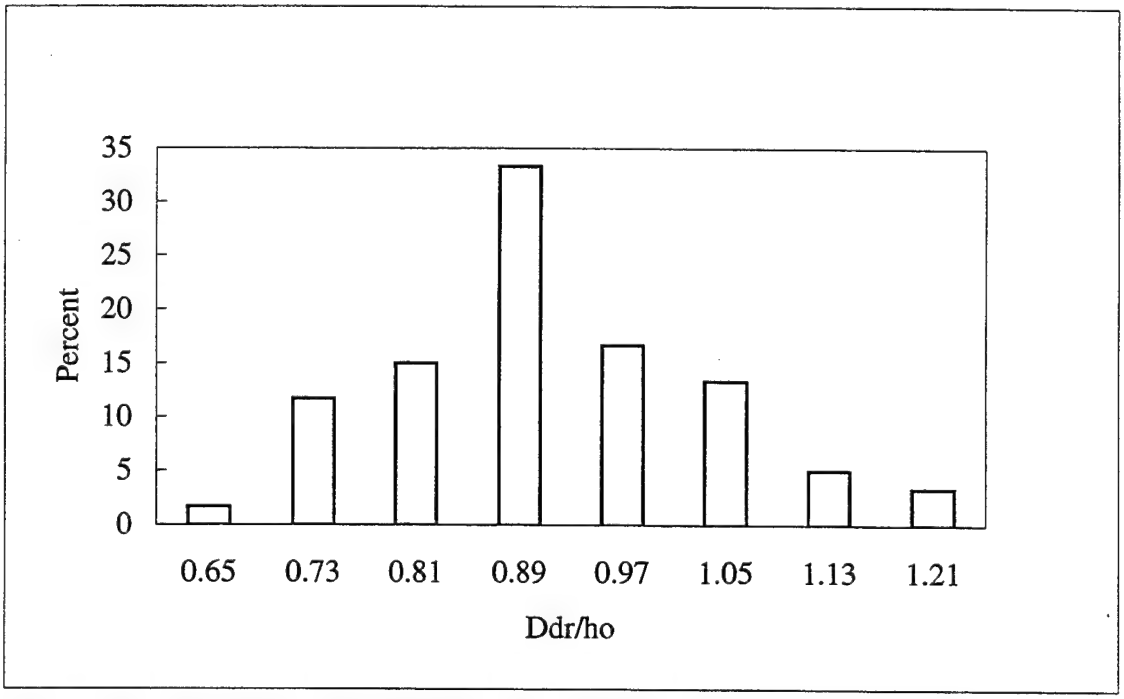

Figure 36. Distribution of normalized drop diameter for fresh water free jet at 10 degree ramp angle (k/ho = 0.06, We = 3014, Fr = 25.8, ho = 5.8 mm).

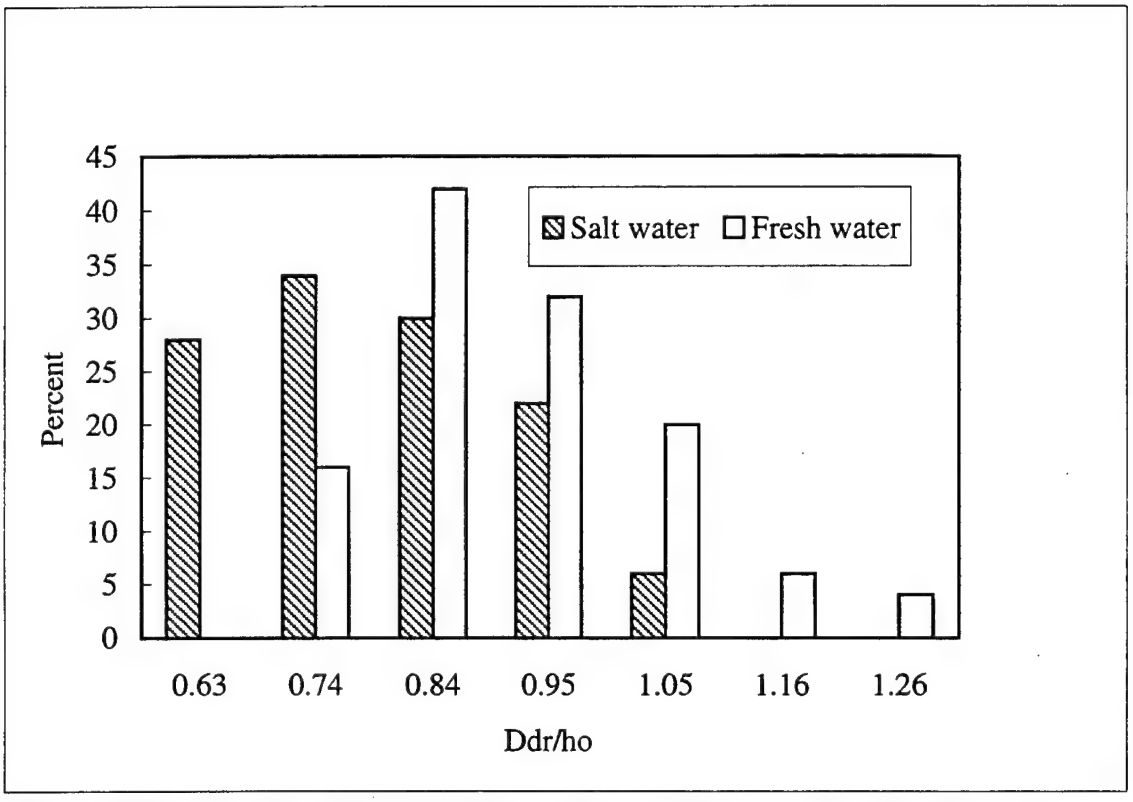

Figure 37. Comparison of the distributions of normalized drop diameter for salt and fresh water free jets at 10 degree ramp angle.

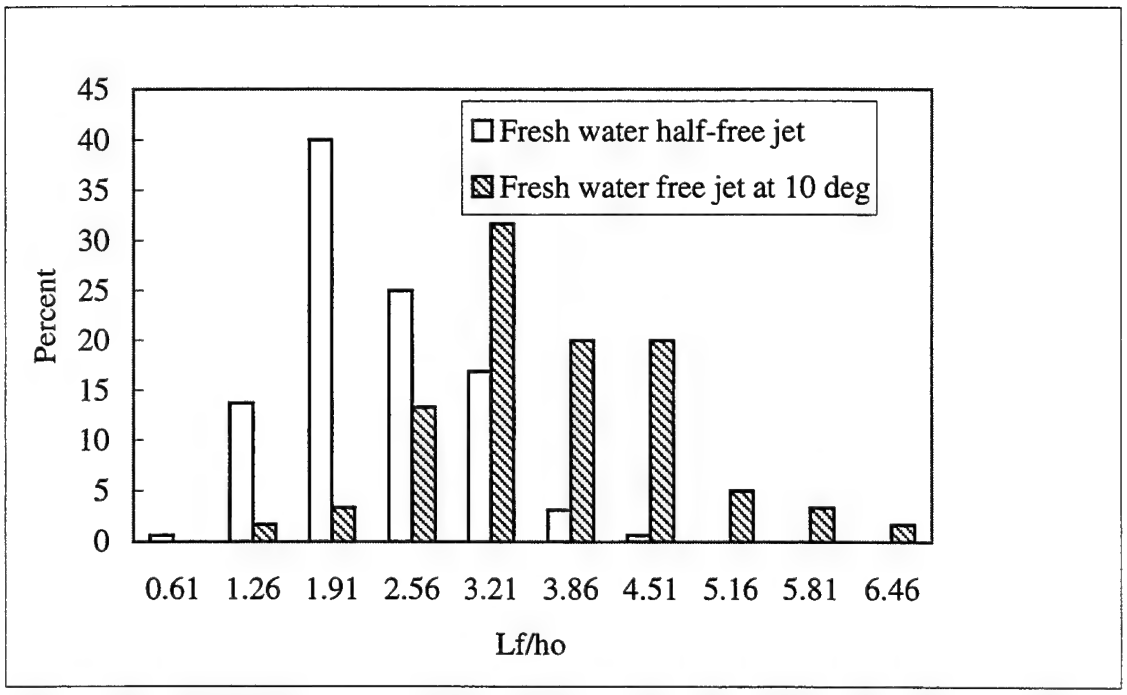

Figure 38a. Distribution of normalized filament length for fresh water half-free and free jets (k/ho = 0.06, We = 3014, Fr = 25.8, ho = 5.8 mm).

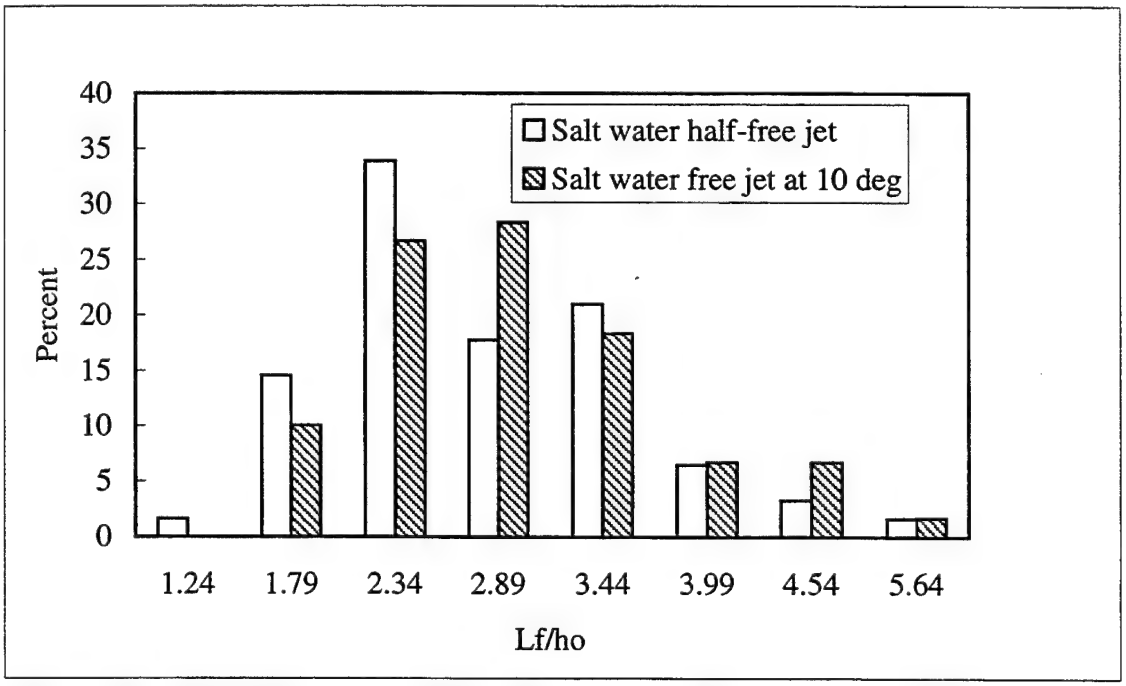

Figure 38b. Distribution of normalized filament length for salt water half-free and free jets (k/ho = 0.06, We = 3095, Fr = 25.8, ho = 5.8 mm).

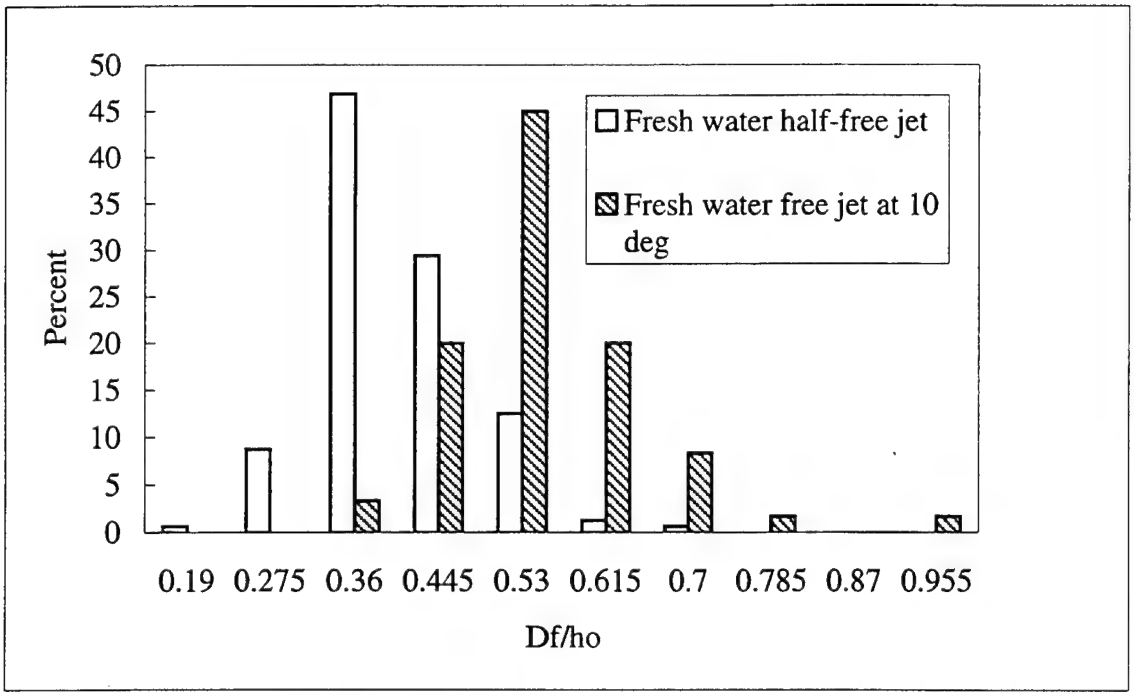

Figure 39a. Distribution of normalized filament diameter for fresh water half-free and free jets (k/ho = 0.06, We = 3014, Fr = 25.8, ho = 5.8 mm).

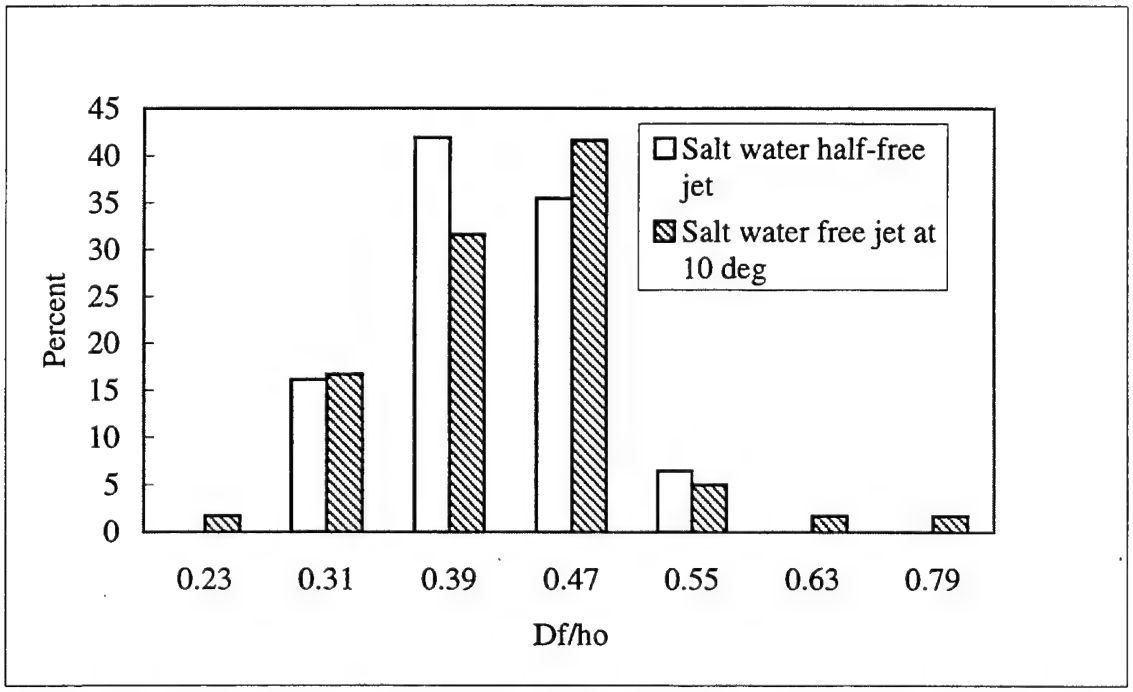

Figure 39b. Distribution of normalized filament diameter for salt water half-free and free jets (k/ho = 0.06, We = 3095, Fr = 25.8, ho = 5.8 mm).

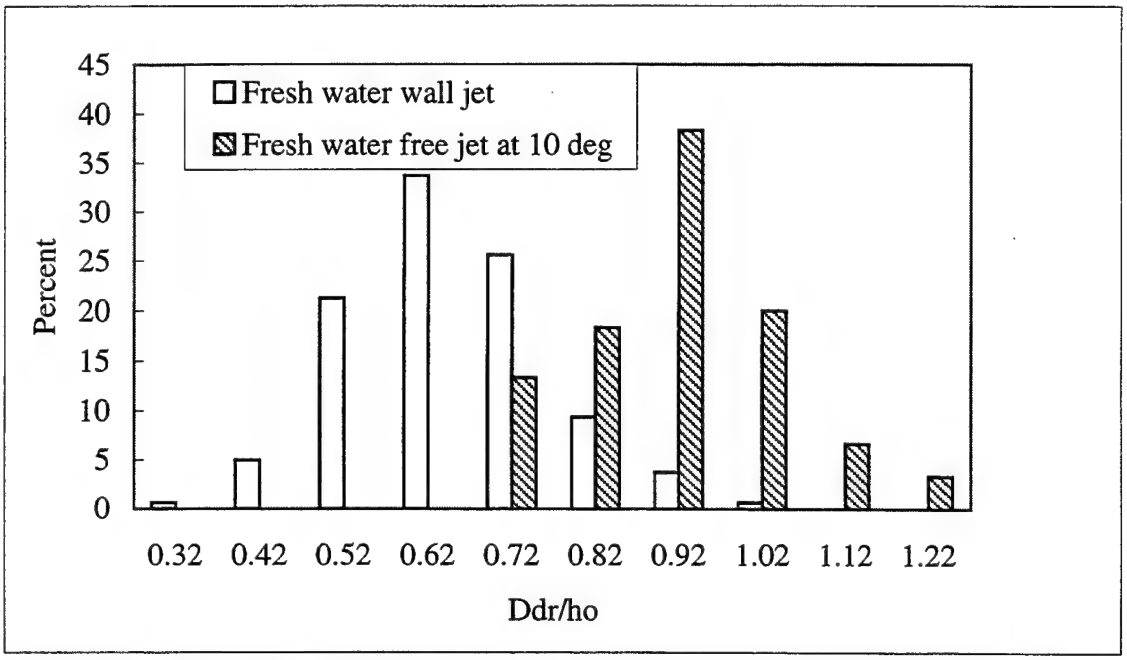

Figure 40a. Distribution of normalized drop diameter for fresh water half-free and free jets (k/ho = 0.06, We = 3014, Fr = 25.8, ho = 5.8 mm).

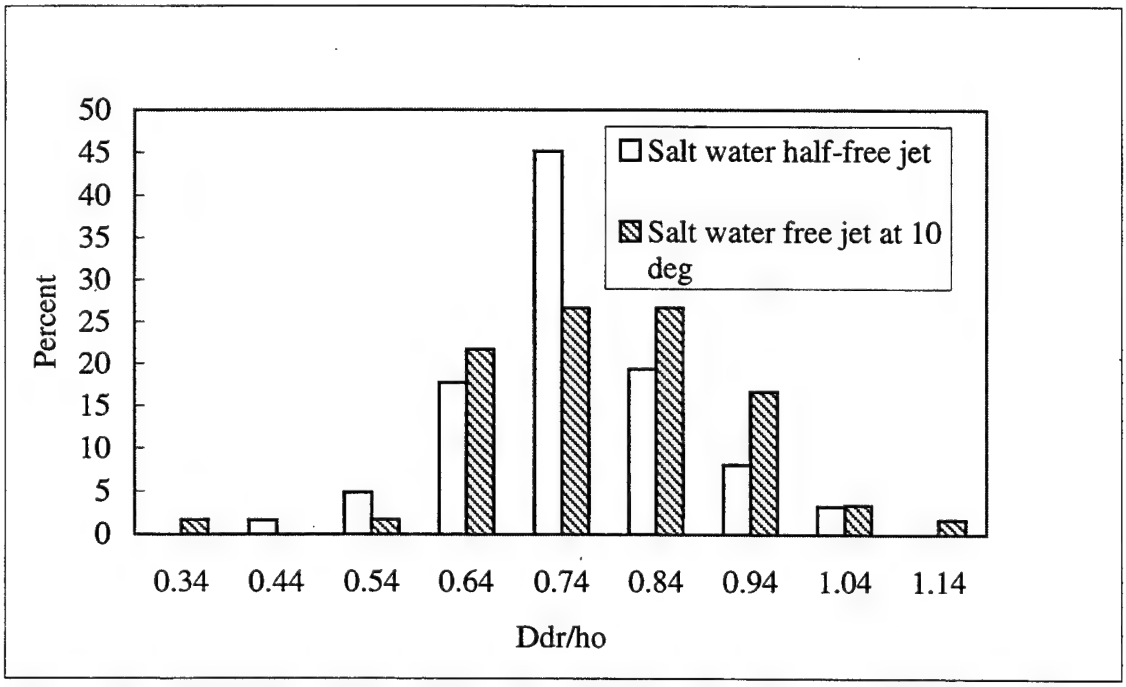

Figure 40b. Distribution of normalized drop diameter for salt water half-free and free jets (k/ho = 0.06, We = 3095, Fr = 25.8, ho = 5.8 mm).

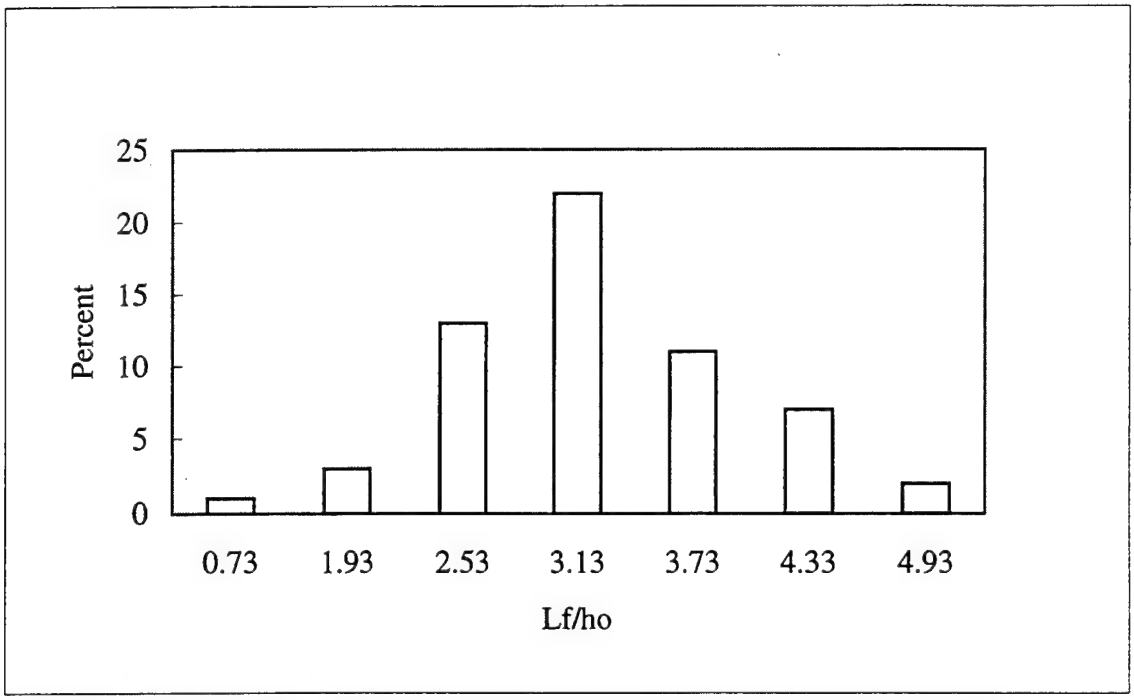

Figure 41. Distribution of normalized filament length for fresh water free jet at 15 degree ramp angle (k/ho = 0.06, We = 3014, Fr = 25.8, ho = 5.8 mm).

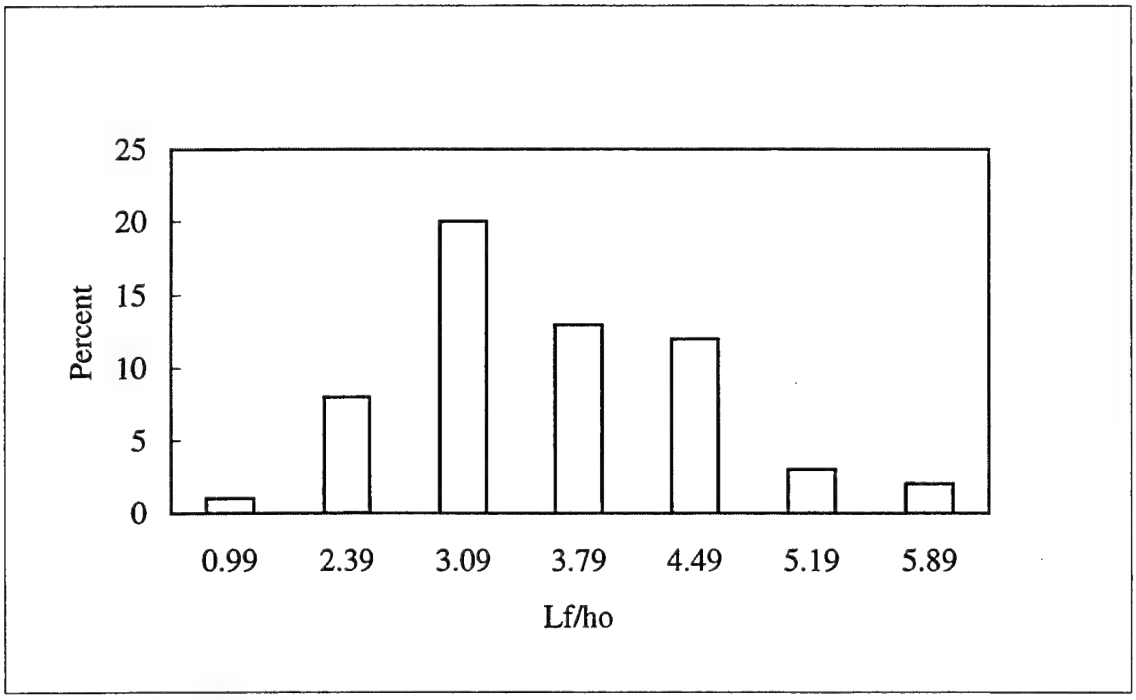

Figure 42. Distribution of normalized filament length for fresh water free jet at 10 degree ramp angle (k/ho = 0.06, We = 3014, Fr = 25.8, ho = 5.8 mm).

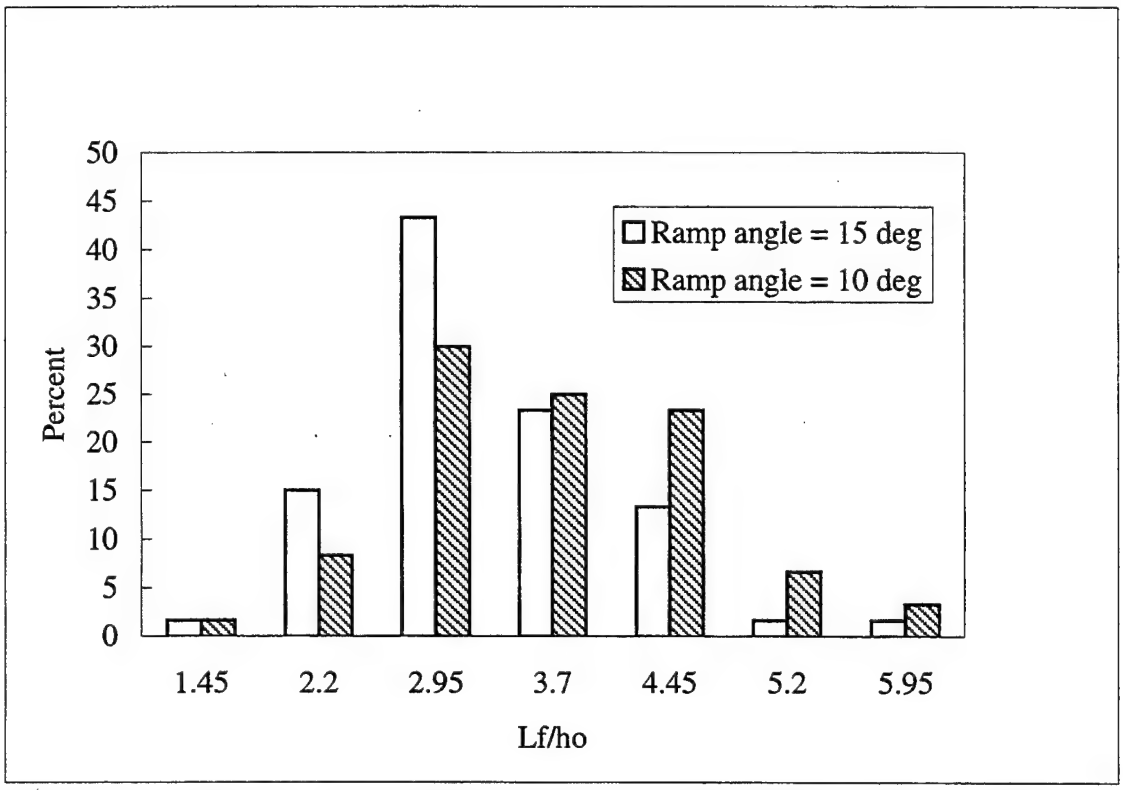

Figure 43. Comparison of the distributions of normalized filament length for fresh water free jet for two different ramp angles.

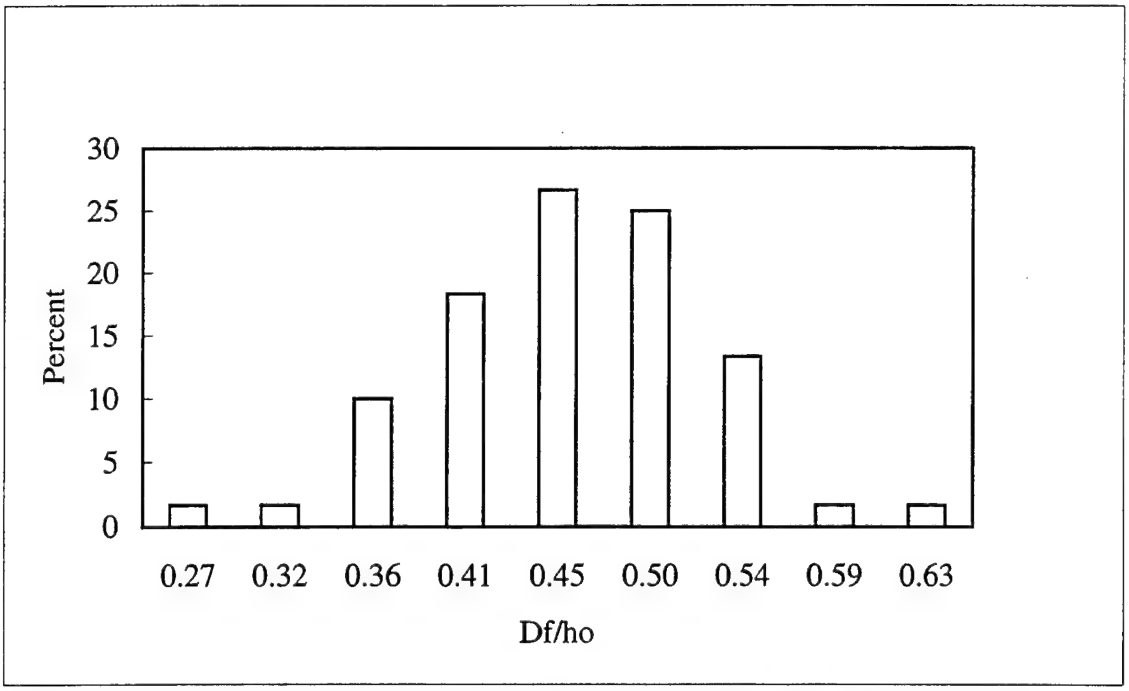

Figure 44. Distribution of normalized filament diameter for fresh water free jet at 15 degree ramp angle (k/ho = 0.06, We = 3014, Fr = 25.8, ho = 5.8 mm).

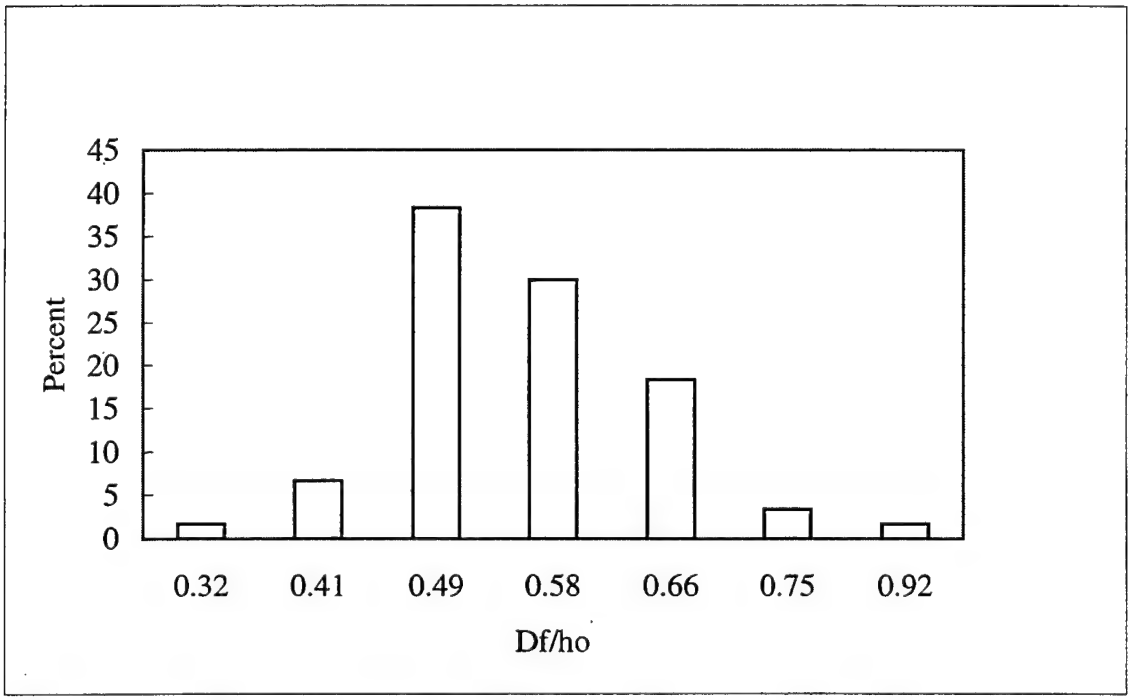

Figure 45. Distribution of normalized filament diameter for fresh water free jet at 10 degree ramp angle (k/ho = 0.06, We = 3014, Fr = 25.8, ho = 5.8 mm).

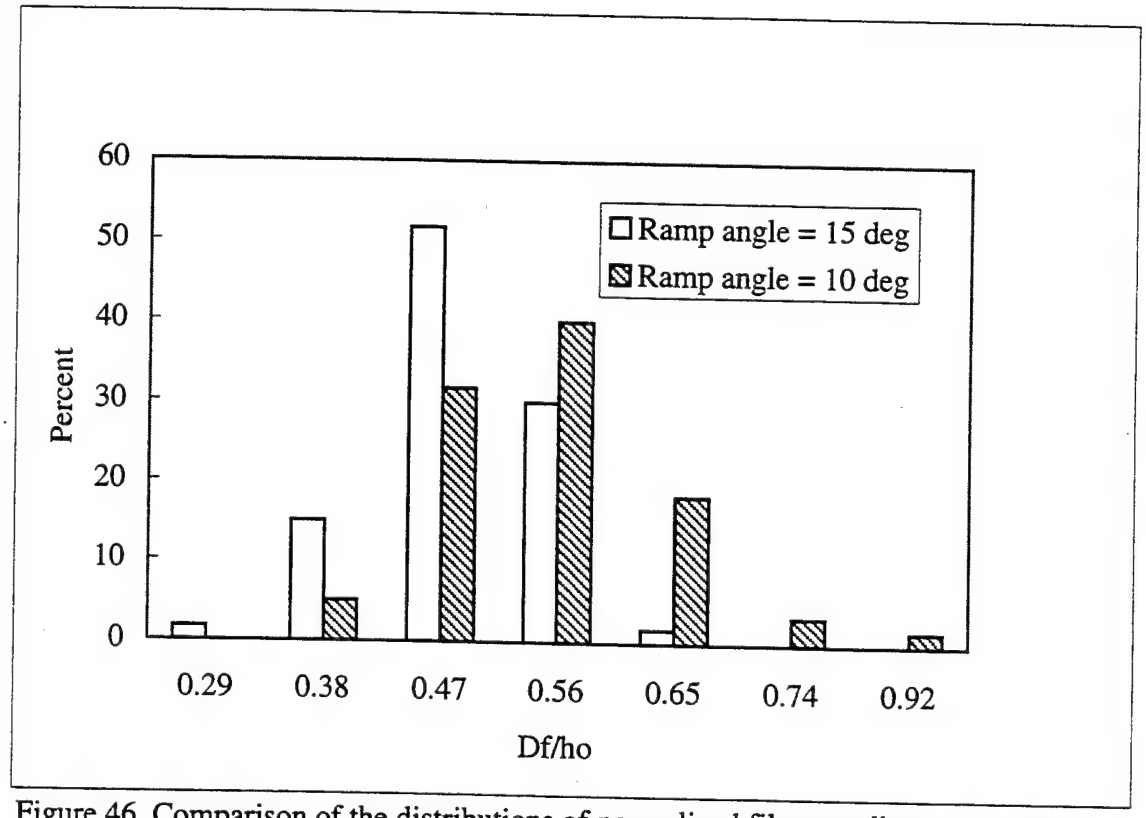

Figure 46. Comparison of the distributions of normalized filament diameter for fresh water free jet at two different ramp angles.

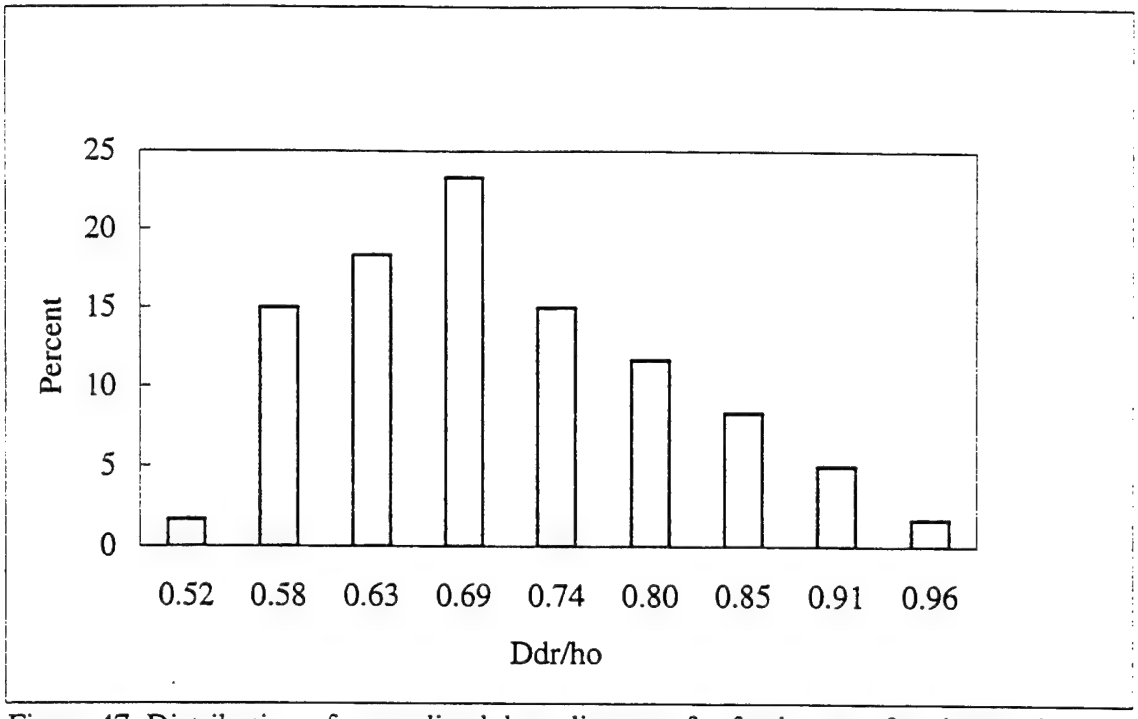

Figure 47. Distribution of normalized drop diameter for fresh water free jet at 15 degree ramp angle (k/ho = 0.06, We = 3014, Fr = 25.8, ho = 5.8 mm).

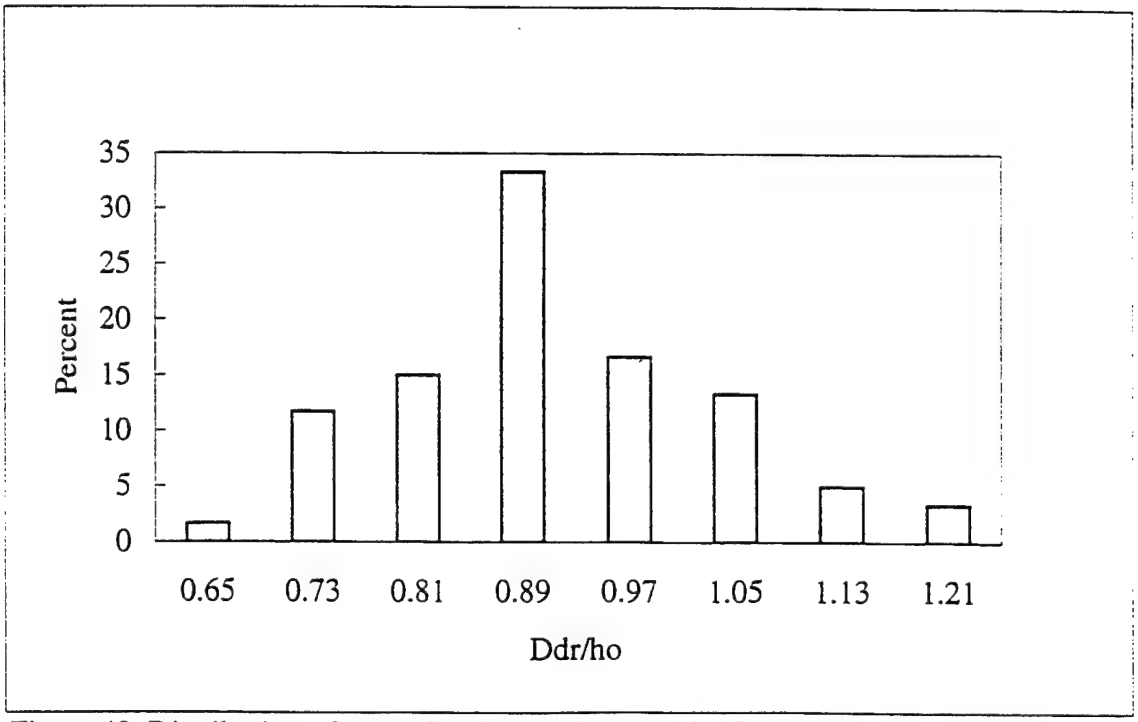

Figure 48. Distribution of normalized drop diameter for fresh water free jet at 10 degree ramp angle (k/ho = 0.06, We = 3014, Fr = 25.8, ho = 5.8 mm).

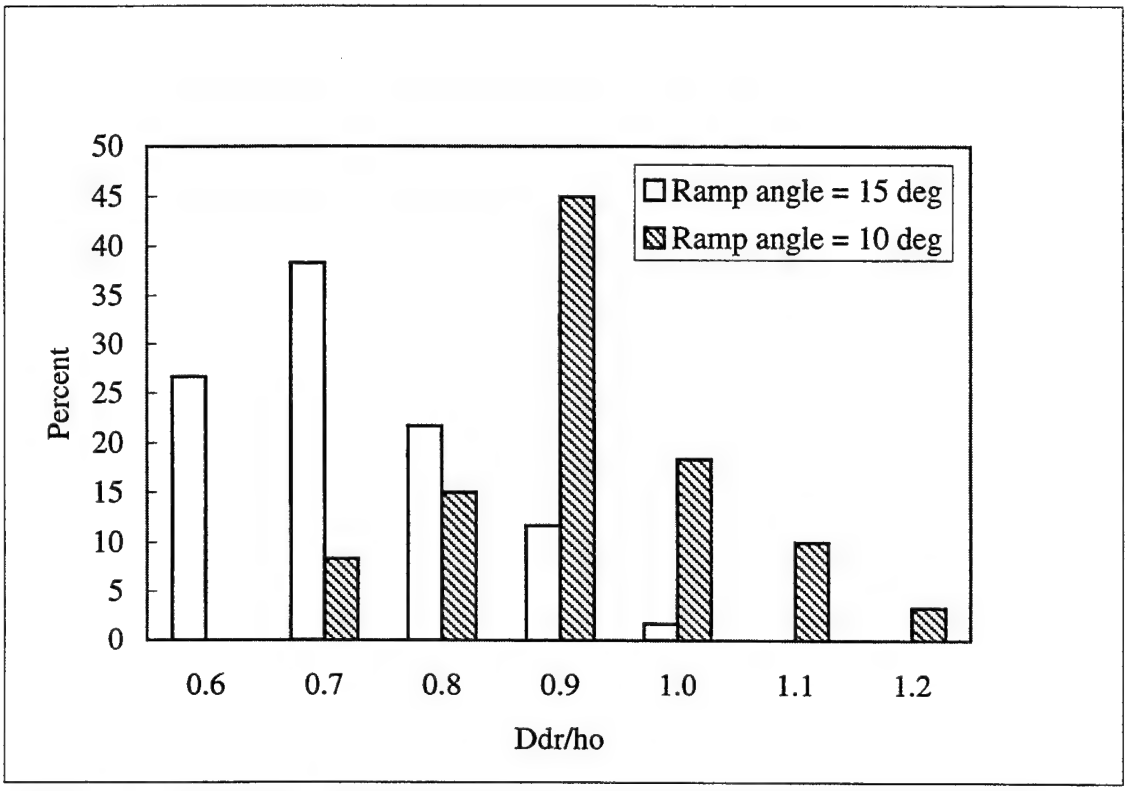

Figure 49. Comparison of the distributions of normalized drop diameter for fresh water free jet at two different ramp angles.

THIS PAGE LEFT INTENTIONALLY BLANK

LIST OF REFERENCES

Dai, Z., Chou, W.-H., and Faeth, G. M. 1998. "Drop formation due to turbulent primary breakup at the free surface of plane liquid wall jets," *Physics of Fluids*, Vol. 10, pp. 1147-1157.

Dombrowski, N. and Fraser, R. P. 1954. "A photographic investigation into the disintegration of liquid sheets," *Philosophical Transactions of the Royal Society of London*, Vol. 247, No. A924, pp. 101-130.

Fiendt, E. G. 1957. "Untersuchungen uber die Abhangigkeit des Umschlages Laminar-Turbulent von der Oberflachenraughigkeit und der Druckverteiling," *Jb. 1956 Schiffbautechn. Ges.*, Vol. 50, pp. 180-203.

Finley, P. J., Khoo, C. P. and Chin, J. P. 1966. "Velocity measurements in a thin turbulent water layer," *La Houille Blanche*, Vol. 21, pp. 713-721.

Grass, A. J. 1971. "Structural features of turbulent flow over smooth and rough boundaries," *Journal of Fluid Mechanics*, Vol. 50, pp. 233-255.

Hoyt, J. W. and Taylor, J. J. 1977a. "Waves on water jets," *Journal of Fluid Mechanics*, Vol. 83, pp. 119-127.

Hoyt, J. W. and Taylor, J. J. 1977b. "Turbulence structure in a water jet discharging in air," *Physics of Fluids*, Vol. 20, Pt. II, No. 10, pp. S253-S257.

Klebanoff, P. S. 1954. "Characteristics of turbulence in a boundary layer with zero pressure gradient," NACA Technical Note 3178.

Ligrani, P. M., Moffat, R. J. and Kays, W. M. 1979. "The thermal and hydrodynamic behavior of thick, rough-wall, turbulent boundary layers," Report HMT-29, Thermosciences Divison, Dept. of Mechanical Engineering, Stanford University.

Lord Rayleigh 1945. "On the instability of jets," *Proceedings of the London Mathematical Society,* Dover Publications, New York, Vol. 10, pp. 4-13.

McCarthy, M. J. and Molloy, N. A. 1974. "Review of stability of liquid jets and the influence of nozzle design," *Chemical Engineering Journal*, Vol. 7, pp. 1-20.

Merrill, C. F. 1998. "Spray Generation from liquid wall jets over smooth and rough surfaces," Phd Dissertation, Mechanical Engineering Naval Post Graduate School, Monterey, CA.

Phiney, R. E. 1973. "The breakup of a turbulent jet in a Gaseous Atmosphere," *Journal of Fluid Mechanics,* Vol. 60, pp. 689-701.

Pimenta, M. M., Moffat, R. J. and Kays, W. M. 1975. "Turbulent boundary layer: an experimental study of the transport of momentum and heat with the effect of roughness," Report HMT-21, Thermosciences Div., Dept. of Mechanical Engineering, Stanford University.

Raupach, M. R. 1981. "Conditional statistics of Reynolds stress in rough-wall and smooth-wall turbulent boundary layers," *Journal of Fluid Mechanics*, Vol. 108, pp. 363-382.

Rein, M. 1996. "The transitional regime between coalescing and splashing drops," *Journal of Fluid Mechanics,* Vol. 306, pp. 145-165.

Rouse, H. and Abol-Fetouh, A.-H. 1950. "Characteristics of irrotational flow through axially symmetric orifices," *Journal of Applied Mechanics*, Vol. 17, pp. 421-426.

Sarpkaya, T. 1977. "In-line and transverse forces on cylinders in oscillatory flow at high Reynolds numbers," *Journal of Ship Research*, Vol. 21, pp. 200-216.

Sarpkaya, T. 1986. "Force on a circular cylinder in viscous oscillatory flow at low Keulegan-Carpenter numbers," *Journal of Fluid Mechanics*, Vol. 165, pp. 61-71.

Schlicting, H. 1979. *Boundary-Layer Theory.* 7th Edition. McGraw-Hill Inc., NY.

Townson, J. M. 1988. *Free Surface Hydraulics,* 1st Edition. Unwin Hyman, London, Chapter 6.

Volkart, P. 1980. "The mechanism of air bubble entrainment in self-aerated flow," *International Journal of Multiphase Flow,* Vol. 6, pp. 411-423.

Wu, P.-K. and Faeth, G. M. 1995. "Onset and end of drop formation along the surface of turbulent liquid jets in still gases," *Physics of Fluids*, Vol. 7, pp. 2915-2917.

INITIAL DISTRIBUTION LIST

1. Defense Technical Information Center 2
   8725 John J. Kingman Rd., STE 0944
   Ft. Belvior, VA 22060-6218

2. Dudley Knox Library 2
   Naval Postgraduate School
   411 Dyer Rd.
   Monterey, CA 93943-5101

3. Department Chairman, Code ME 2
   Department of Mechanical Engineering
   Naval Postgraduate School
   Monterey, CA 93943-5000

4. Professor T. Sarpkaya, Code ME-SL 5
   Department of Mechanical Engineering
   Naval Postgraduate School
   Monterey, CA 93943-5000

5. Curricular Officer, Code 34 1
   Naval Engineering Department
   Naval Postgraduate School
   Monterey, CA 93943-5000

6. Commanding Officer 3
   PMOSSP Sunnyvale
   PO Box 391537
   Mountain View, CA 94039-1537
   ATTN: LT Rajan Vaidyanathan